Atmos. Chem. Phys. Discuss., doi:10.5194/acp-2016-782, 2016
Manuscript under review for journal Atmos. Chem. Phys.
Published: 9 September 2016

Atmospheric Chemistry and Physics Discussions

Sensitivity of black carbon concentrations and climate impact to aging and scavenging

Marianne T. Lund[1,*], Terje K. Berntsen[1,2], Bjørn H. Samset[1]

1 CICERO - Center for International Climate and Environmental Research, Oslo, Norway

2 Department of Geosciences, University of Oslo, Oslo, Norway

**Corresponding author, m.t.lund@cicero.oslo.no, Phone: +47 22 85 86 94*

Abstract

Despite recent improvements, significant uncertainties in global modeling of black carbon (BC) aerosols persist, posing important challenges for the design and evaluation of effective climate mitigation strategies targeted at BC emission reductions. Here we investigate the sensitivity of BC concentrations in the chemistry-transport model OsloCTM2 with the microphysical aerosol parameterization M7 (OsloCTM2-M7) to parameters controlling aerosol aging and scavenging. We focus on Arctic surface concentrations and remote region BC vertical profiles, and introduce a novel treatment of condensation of nitric acid on BC.

The OsloCTM2-M7 underestimates annual averaged BC surface concentrations, with a mean normalized bias of -0.55. The seasonal cycle and magnitude of Arctic BC surface concentrations is improved compared to previous OsloCTM2 studies, but model-measurement discrepancies during spring remain. High-altitude BC over the Pacific is overestimated compared with measurements from the HIPPO campaigns. We find that a shorter global BC lifetime improves the agreement with HIPPO, in line with other recent studies. Several processes can achieve this, including allowing for convective scavenging of hydrophobic BC and reducing the amount of soluble material required for aging. Simultaneously, the concentrations in the Arctic are reduced, resulting in poorer agreement with measurements in part of the region.

A first step towards inclusion of aging by nitrate in OsloCTM2-M7 is made by allowing for condensation of nitric acid on BC. This results in a faster aging and reduced lifetime, and in turn to a better agreement with the HIPPO measurements. On the other hand, model-

Atmos. Chem. Phys. Discuss., doi:10.5194/acp-2016-782, 2016
Manuscript under review for journal Atmos. Chem. Phys.
Published: 9 September 2016

measurement discrepancies in the Arctic are exacerbated. Work to further improve this parameterization is needed.

The impact on global mean radiative forcing (RF) and surface temperature response (TS) in our experiments is estimated. Compared to the baseline, decreases in global mean direct RF on the order of 10-30% of the total pre-industrial to present BC direct RF is estimated for the experiments that result in the largest changes in BC concentrations.

We show that globally tuning parameters related to BC aging and scavenging can improve the representation of BC vertical profiles in the OsloCTM2-M7 compared with observations. Our results also show that such improvements can result from changes in several processes and often depend on assumptions about uncertain parameters such as the BC ice nucleating efficiency and the change in hygroscopicity with aging. It is also important to be aware of potential tradeoffs in model performance between different regions. Other important sources of uncertainty, particularly for Arctic BC, such as model resolution has not been investigated here. Our results underline the importance of more observations and experimental data to improve process understanding and thus further constrain models.

1 Introduction

Black carbon (BC) aerosols play an important role in the climate system through several mechanisms including direct absorption of solar radiation (Bond et al., 2013; Myhre et al., 2013), changing surface albedo (Flanner et al., 2009; Warren & Wiscombe, 1980), modification of cloud properties and thermal stability (Koch & Del Genio, 2010; Lohmann & Feichter, 2005), and influence on precipitation and circulation (Bollasina et al., 2014; Wang et al., 2015). The potentially strong climate warming, combined with short atmospheric residence time and harmful health impacts (Anenberg et al., 2012; Aunan et al., 2006; Shindell et al., 2011), has made BC reductions an attractive mitigation measure (AMAP, 2015; Bowerman et al., 2013; EPA, 2012; Grieshop et al., 2009; Kopp & Mauzerall, 2010; UNEP/WMO, 2011).

However, accurately representing the distribution of BC concentrations in global atmospheric models remains challenging and considerable inter-model variability and model-measurement discrepancies exist. In particular two features have been pointed out in several studies:

Atmos. Chem. Phys. Discuss., doi:10.5194/acp-2016-782, 2016
Manuscript under review for journal Atmos. Chem. Phys.
Published: 9 September 2016

Atmospheric Chemistry and Physics Discussions

underestimation of the magnitude and difficulty capturing the seasonal cycle of Arctic BC surface concentrations (e.g., (Eckhardt et al., 2015; Shindell et al., 2008)) and an overestimation of high altitude BC concentrations over remote regions (e.g., (Koch et al., 2009b; Lee et al., 2013; Samset et al., 2014; Schwarz et al., 2013; Wang et al., 2014)). Because the impact of the aerosols on radiation and temperature depends strongly on altitude, such discrepancies lead to uncertainties in the net climate impact of BC. While overestimating high altitude BC concentrations can result in an overestimation of the BC radiative forcing (Samset & Myhre, 2011), too low surface concentrations may lead to an underestimation of the temperature response due to the reduced efficacy of BC forcing with altitude (Ban-Weiss et al., 2011; Flanner, 2013; Samset & Myhre, 2015). This in turn poses significant challenges for the design and evaluation of effective BC mitigation strategies.

Several studies have explored how scavenging processes and uncertainties in emissions contribute to the inter-model and model-measurement discrepancies. Some have investigated how these processes influence transport of BC to the Arctic (Bourgeois & Bey, 2011; Browse et al., 2012; Liu et al., 2011), others have focused on the vertical BC distribution in remote regions (Fan et al., 2012; Hodnebrog et al., 2014; Kipling et al., 2016; Kipling et al., 2013).

In this study we use the chemical transport model OsloCTM2 (Sovde et al., 2008) with the microphysical aerosol parameterization M7 (Vignati et al., 2004) (hereafter OsloCTM2-M7) to investigate the sensitivity of modeled BC concentrations to changes in a range of parameters related to aging and scavenging processes and how these influence the model-measurement discrepancies, focusing simultaneously on Arctic surface concentrations and remote region vertical distributions of BC.

The OsloCTM2 has been used in several multi-model studies of aerosol impacts (Balkanski et al., 2010; Myhre et al., 2013; Schulz et al., 2006; Shindell et al., 2013; Textor et al., 2007). These studies used a simplified bulk parameterization of carbonaceous aerosols. Lund and Berntsen (2012) compared the M7 to this bulk parameterization and found improved representation of modeled BC seasonal cycle and magnitude at high latitudes. However, a comparison against BC vertical profiles measured during one aircraft campaign suggested that M7 exacerbated high-altitude overestimation of concentrations.

Here we use updated inventories of anthropogenic and biomass burning emissions and three years of model results, and further evaluate the OsloCTM2-M7 against a range of observations

Atmos. Chem. Phys. Discuss., doi:10.5194/acp-2016-782, 2016
Manuscript under review for journal Atmos. Chem. Phys.
Published: 9 September 2016

Atmospheric Chemistry and Physics Discussions

from surface stations, flight campaigns, and snow samples. Next, we perform sensitivity experiments to quantify the impact of changes in a range of physical and microphysical parameters on the BC distribution. Our sensitivity experiments include a first step towards accounting for gas-phase nitric acid condensation in the BC aging parameterization. Measurements have shown that nitrate is frequently present in internal aerosol mixtures and contribute to the aging of BC (Pratt & Prather, 2010; Shiraiwa et al., 2007), a process currently excluded in many models. This process may also become more important in the future following strong projected decreases in SO_2 emissions and increasing NOx and greenhouse gas emissions (Bauer et al., 2007; Bellouin et al., 2011; Makkonen et al., 2012). Finally, we estimate the subsequent impact of BC concentrations changes on global radiative forcing and surface temperature response.

Section 2 describes the model setup and experiments, Sect. 3 presents and discusses results and Sect. 4 gives the conclusions.

2 Methodology

2.1 The OsloCTM2-M7

The OsloCTM2 is a global off-line 3-dimensional chemistry transport model with transport driven by meteorological data generated by the Integrated Forecast System (IFS) model at the European Center for Medium Range Weather Forecast (ECMWF) (Sovde et al., 2008). The model is run for 2008-2010 with a T42 resolution (approximately 2.8° x 2.8°) and 60 vertical layers from the surface to 0.1 hPa.

The microphysical aerosol module M7 (Lund & Berntsen, 2012; Vignati et al., 2004) includes the main aerosol species sea salt, mineral dust, sulfate and organic carbon, in addition to BC. Aerosols are represented by seven modes with size distribution given by a lognormal distribution function. BC aerosols are separated into soluble (mixed) and insoluble particles and can exist in the Aitken, accumulation and coarse modes. BC aerosols are assumed to be 100% hydrophobic and in the Aitken mode upon emission. Aging then occurs due to condensation of sulfuric acid produced in the gas-phase reaction $OH+SO_2 \rightarrow H_2SO_4$ or coagulation with sulfate particles. M7 is coupled to the sulfur/oxidant chemistry in the OsloCTM2, i.e., the production of sulfate is explicitly calculated and is dependent on the SO_2 emissions and oxidant levels and thus variable in time and space.

Atmos. Chem. Phys. Discuss., doi:10.5194/acp-2016-782, 2016
Manuscript under review for journal Atmos. Chem. Phys.
Published: 9 September 2016

Particles in the soluble modes are assumed to be hygroscopic and are removed according to the fraction of the liquid plus ice water content of a cloud that is removed by precipitation (Berntsen et al., 2006), assuming 100% scavenging efficiency by both water and ice in both large-scale and convective precipitation in the baseline setup. Since Lund and Berntsen (2012) the temporal frequency of wet scavenging in OsloCTM2-M7 has been reduced from three to one hour. The dry deposition velocities for all aerosols depends on particle size and density, turbulence close to surface and the resistance of the laminar sub layer (Grini, 2007). The OsloCTM2-M7 also keeps track of the BC concentration in snow. Snow depth and snowfall data from ECMWF is used to build snow layers in the model and BC is dry and wet deposited in these. For detailed description see Appendix A of Skeie et al. (2011).

The sulfate and nitrate modules are described in detail in Berglen et al. (2004) and Myhre et al. (2006), and we only give brief summaries here.

The sulfur cycle chemistry scheme includes dimethyl sulfide (DMS), SO_2, sulfate, H_2S and methane sulfonic acid (MSA) and the concentrations of sulfur is calculated interactively with the oxidant chemistry. Gas-phase oxidation of SO_2 by OH forms sulfate and SO_2 is also oxidized to aqueous phase sulfate by H_2O_2, HO_2NO_2 and O_3. When M7 is used, the gas-phase sulfate is saved in a separate tracer and allowed to condense on the insoluble aerosol modes. The aqueous phase sulfate is transferred to the accumulation and coarse mode sulfate tracers in M7 according to a prescribed fraction. The treatment of sulfate aerosols then follows M7.

The chemical equilibrium of semi-volatile inorganic species is treated with the Equilibrium Simplified Aerosol model (EQSAM) (Metzger et al., 2002a; Metzger et al., 2002b). EQSAM considers the $NH_4^+/Na^+/SO_4^{2-}/NO_3^-/Cl^-/H_2O$ system and calculates the gas/aerosol partitioning of ammonium nitrate under the assumption that aerosols are internally mixed and obey thermodynamic gas/aerosol equilibrium. Nitrate aerosol is represented by two modes; a fine mode comprised of sulfate and a coarse mode comprised of sea salt. After H_2SO_4 and HNO_3 have been generated by the photochemistry, the thermodynamic equilibrium is solved using EQSAM.

2.2 Emissions

Anthropogenic emissions for 2008-2010 are from the ECLIPSEv4 inventory developed with the GAINS model (Amman et al. 2011) as part of the activities under the ECLIPSE project funded by the European Commission 7th Framework (Amann et al., 2011; Klimont et al., 2009;

Atmos. Chem. Phys. Discuss., doi:10.5194/acp-2016-782, 2016
Manuscript under review for journal Atmos. Chem. Phys.
Published: 9 September 2016

Atmospheric Chemistry and Physics Discussions

Klimont et al., 2016) (available upon request from http://eclipse.nilu.no/). Emissions from international shipping and aviation are from the Representative Concentration Pathway (RCP) 6.0 (Fujino et al., 2006; Hijioka et al., 2008). Biomass burning emissions are from the Global Fire Emission Database version 3 (GFEDv3) (van der Werf et al., 2010). Seasonal variability in domestic emissions is accounted for by using monthly weights (2000-2006 average) for each grid based on spatially distributed temperature data from the Climate Research Unit (CRU) following the methodology described in Streets et al. (2003). Total BC emissions in 2010 are 5866 Gg from fossil fuel plus biofuel sources and 2273 Gg from biomass burning.

2.3 Experiments

We first perform a three-year base simulation with meteorological data and emissions for 2008-2010, which forms the basis for the model evaluation. Next, we perform a range of sensitivity experiments described in the following paragraphs and summarized in Table 1.

Several sensitivity experiments are related to the aging of BC. First, we explore the impact of varying the amount of soluble material required to transfer the BC aerosols to the soluble mode. The M7 uses the concept of monolayers (ML); when sufficient soluble material is associated with a hydrophobic particle to form "n" monomolecular layers around the particle, the particle is assumed to be hygroscopic and is transferred to the mixed mode. Currently, n=1 is used based on the best agreement with a sectional model found by Vignati et al. (2004). However, the amount of soluble material required for a particle to become hygroscopic is an important source of uncertainty (Vignati et al., 2010). Popovicheva et al. (2011) used a laboratory approach to quantify the water uptake by particles with varying amounts of sulfates in order to simulate the aging of combustion particles. Based on a quantification measure for separating hygroscopic and non-hygroscopic soots (Popovicheva et al., 2008), the laboratory results suggest that the transformation of soot particles from hydrophobic to hydrophilic requires an H_2SO_4 surface coverage of 0.5-1.4 ML, while 1.4-2.3 ML were required for transformation to hygroscopic mode. Based on these results we perform three model simulations assuming 0.5, 1.4 and 2.3 ML required for BC aging. Next, we perform a test where 50% of BC from biomass burning sources is emitted directly in the accumulation mode instead of in the insoluble Aitken mode. This is based on observational evidence suggesting that biomass burning BC tends to be larger and more aged, with thicker coatings than BC from urban source (Schwarz et al., 2008). Finally, we test the impact of allowing for BC aging by condensation of nitric acid (HNO_3), first including total HNO_3 and then excluding HNO_3 produced in the aqueous-phase reaction with

Atmos. Chem. Phys. Discuss., doi:10.5194/acp-2016-782, 2016
Manuscript under review for journal Atmos. Chem. Phys.
Published: 9 September 2016

Atmospheric Chemistry and Physics Discussions

N_2O_5. We extend, in a simplified manner, M7 to also account for condensation by HNO_3 on insoluble particles after gas/aerosol partitioning with ammonium-nitrate is calculated in EQSAM. We follow the same treatment of condensation as for sulfate in M7 (Vignati et al., 2004) and adopt an accommodation coefficient for HNO_3 of 0.1 (Pringle et al., 2010). Three different runs are performed where the number of required ML are assumed to be one (as for sulfate in the standard M7 case), five or ten. Results presented in Sect. 3 uses ML=5.

The second set of sensitivity tests is related to emissions and wet scavenging, the main loss mechanism of BC and hence a key parameter for the lifetime and distribution. Hydrophilic BC is originally assumed to be 100% removed by both liquid and ice in large-scale mixed-phase clouds in the OsloCTM2-M7. However, this high efficiency of BC removal by ice-phase precipitation is uncertain. Koch et al. (2009a) found that assuming 12% ice removal of BC gave optimal agreement with observations. This fraction was also supported by observations in Cozic et al. (2007) and has been adopted in studies with the OsloCTM2 bulk aerosol parameterization (e.g. Skeie et al. (2011)). Here we compare results with 100% and 12% removal efficiency for large-scale ice-phase clouds. The removal scheme in OsloCTM2-M7 also assumes no wet scavenging of hydrophobic particles. However, hydrophobic BC aerosol may still be subject to removal by impact scavenging or act as ice nuclei (IN) in convective and mixed-phase clouds (Ekman et al., 2006; Kajino et al., 2012; Park et al., 2005). The BC IN activity is not well known. In order to represent at least some of this uncertainty, we perform two sensitivity tests assuming either 100% or 20% removal efficiency of hydrophobic BC by convective precipitation, with the latter loosely based onHoose et al. (2010). We also perform a combination test assuming 12% removal efficiency of hydrophilic BC by large-scale ice-phase clouds and 20% removal of hydrophobic BC by convective precipitation.

Finally, we perform two additional tests to investigate the impact of seasonality in domestic and agricultural waste burning emissions and higher emissions in Russia following a recent study by Huang et al. (2015). In the first, we alternately remove the seasonal variation in domestic and agricultural waste burning emissions, while in the second the ECLIPSEv4 emissions in Russia are replaced by Huang et al. (2015). These have limited impact on the global BC distributions, but their influence on the seasonal cycle of Arctic BC concentrations is discussed in Sect. 3.1.1.

TABLE 1

Atmos. Chem. Phys. Discuss., doi:10.5194/acp-2016-782, 2016
Manuscript under review for journal Atmos. Chem. Phys.
Published: 9 September 2016

Atmospheric Chemistry and Physics Discussions

2.4 Radiative forcing and temperature response

To estimate implications of the concentration changes in our experiments for the global BC climate impact, we use 3-dimensional, temporally varying radiative forcing (RF) and surface temperature response (TS) kernels derived from simulations with the CESM-CAM4, where a uniform BC burden was systematically added to each model layer to investigate the climate response to a BC perturbation at a given altitude (Samset & Myhre, 2015). Because the BC perturbations were applied uniformly throughout a single model layer, the temperature response at each grid point is caused partly by the BC forcing exerted locally and partly by forcing in surrounding gridboxes. For each experiment, we therefore multiply the globally averaged vertical BC profile from the OsloCTM2-M7 with the globally averaged forcing and temperature change kernels, respectively. Both direct and semi-direct effects due to aerosol-radiation interactions are included in the kernel response. In line with the nomenclature of the IPCC Fifth Assessment Report we refer to the net effect as effective radiative forcing (ERFari) and the direct effect only as RFari.

CAM4 does not account for the absorption enhancement due to BC aging, resulting in a lower direct RF per BC burden than earlier studies, especially at higher altitudes (e.g., Samset and Myhre (2011)). The consequent temperature response per unit BC may also be underestimated. However, here we focus on the changes from the baseline in each sensitivity experiment rather than absolute climate impacts.

2.5 Observations

Modeled concentrations are evaluated against measurements from surface stations, flight campaigns and snow pack samples.

Measured surface concentrations of BC, sulfate, nitrate, sulfur dioxide and nitric acid across North America are from the IMPROVE and CASTNET networks, while measurements across Europe and the rest of the world are from the EBAS and NOAA GMD databases. We also compare against measurements in China from Zhang et al. (2012) and from Aerosol Mass Spectrometer (AMS) campaigns summarized in Zhang et al. (2007).

To evaluate the model performance we calculate the correlation coefficient and the mean normalized bias (MNB). The MNB for each species is given by Equation 1:

Atmos. Chem. Phys. Discuss., doi:10.5194/acp-2016-782, 2016
Manuscript under review for journal Atmos. Chem. Phys.
Published: 9 September 2016

Atmospheric Chemistry and Physics Discussions

$$MNB = \frac{1}{N}\sum\left(\frac{C_{mod}-C_{obs}}{C_{obs}}\right) \quad (1)$$

where C_{mod} and C_{obs} is modeled and observed concentration and N is the total number of observations.

Following the recommendations by Petzold et al. (2013) observational data are referred to as equivalent BC (EBC), refractory BC (rBC) or elemental carbon (EC) depending on whether measurements are derived from optical absorption methods, incandescence methods or methods that specify the carbon content in carbonaceous matter. To convert to BC concentrations we adopt a mass-absorption cross-section (MAC) of 9.7 m^2/g (Bond & Bergstrom, 2006) for all stations except Alert and Zeppelin, where we use the MAC given in Lee et al. (2013).

BC in snow is compared to snow sample measurements across the Arctic in 2008/2009 (Doherty et al., 2010) and across Northern China in 2010 and 2012 (Wang et al., 2013; Ye et al., 2012). In the latter case, model results for 2010 are used.

Vertical profiles of modeled BC is compared with measurements from several flight campaigns, including ARCPAC (Aerosol, Radiation, and Cloud Processes affecting Arctic Climate), ARCTAS (Arctic Research of the Composition of the Troposphere from Aircraft and Satellites), HIAPER Pole-to-Pole Observations (HIPPO) and A-FORCE (Aerosol Radiative Forcing in East Asia). During ARCPAC and ARCTAS, flights were made across Alaska and Canadian Arctic in spring and summer of 2008 (Brock et al., 2011; Jacob et al., 2010), while HIPPO measured atmospheric constituents along transects from approximately pole-to-pole over the Pacific Ocean during different seasons from 2009 to 2011 (Wofsy et al., 2011). The A-FORCE campaign sampled air masses around Japan in March-April 2009 (Oshima et al., 2012). Data from ARCPAC, ARCTAS and HIPPO is available online from www.esrl.noaa.gov/csd/projects/arcpac/, www.air.larc.nasa.gov/missions/arctas/arctas.html and hippo.ornl.gov/. Data from A-FORCE was provided by Professor Yutaka Kondo, University of Tokyo (personal communication). Model data is also compared with CO concentrations measured during the campaigns.

Model data is interpolated in time and space and extracted along the flight track. An average profile for each campaign and latitude band is calculated by averaging observations and model results in 100 hPa altitude bins (25 hPa for HIPPO data between 400 and 200 hPa). The HIPPO data is also separated into five latitude bands. To evaluate the model performance in each

Atmos. Chem. Phys. Discuss., doi:10.5194/acp-2016-782, 2016
Manuscript under review for journal Atmos. Chem. Phys.
Published: 9 September 2016

Atmospheric Chemistry and Physics Discussions

experiment, we calculate the MNB for each campaign following Eq. 1, where N is determined by the number of altitude and latitude bins.

3 Results and discussion

3.1 Model evaluation

We first evaluate the general performance of the OsloCTM2-M7. While the main focus of this paper is BC, the evaluation is extended to include species relevant for the BC aging process, including sulfate and sulfur dioxide. We also look at the modeled CO distribution. CO is another product of incomplete combustion and therefore has many of the same emission sources as BC. However, due to the longer lifetime of CO a comparison with observations, in particular in the more remote regions mainly influenced by long-range transport, can give an indication of how well the model represents the atmospheric transport.

3.1.1 Surface concentrations

Figure 1 shows annual mean (year 2008) modeled and measured surface concentrations of BC, sulfate, nitrate, sulfur dioxide and nitric acid.

FIGURE 1

The OsloCTM2-M7 underestimates BC and sulfate surface concentrations, with MNB of -0.55 and -0.45, respectively. The underestimation is largest for measurements in China. Nitrate concentrations are in better agreement with measurements, with MNB of 0.08. The model overestimates surface concentrations of sulfur dioxide, especially in Europe, with MNB of 0.70. This may be due to too inefficient conversion to sulfate, which is supported by the underestimation of sulfate aerosols, and/or an overestimation of emissions. Also nitric acid concentrations in Europe and North America are overestimated (MNB 0.75).

We also investigate the seasonal cycle of BC. Figure 2 shows monthly mean modeled BC and measured EBC surface concentrations averaged over 2008-2010. The model captures the magnitude relatively well at Mace Head, Cape Point, Trinidad Head, Barrow and Pallas, but fail to capture some of features of the seasonal variation. Concentrations are also underestimated at Lulin, Hohenpeissenberg and Jungfraujoch during winter and spring.

FIGURE 2

Atmos. Chem. Phys. Discuss., doi:10.5194/acp-2016-782, 2016
Manuscript under review for journal Atmos. Chem. Phys.
Published: 9 September 2016

Many models typically struggle to capture the seasonal cycle and magnitude of measured high-latitude BC surface concentrations. While there has been considerable progress and current models capture high-latitude seasonality better than previous generations (Breider et al., 2014; Browse et al., 2012; Liu et al., 2011; Sharma et al., 2013), problems remain. This is also the case for the OsloCTM2-M7. Lund and Berntsen (2012) showed that inclusion of aerosol microphysics significantly improved both magnitude and seasonality of Arctic BC. This is further improved by the use of updated emissions in the current study, partly due to the inclusion of emissions from flaring, which is an important local Arctic source of BC (Stohl et al., 2013). However, the model still underestimates concentrations during spring. The seasonal variability in emissions is an important factor. Accounting for seasonality in domestic BC emissions in the ECLIPSEv4 inventory increases the burden of total fossil fuel plus biofuel BC north of 65°N by approximately 15% during winter and by 2% on annual average compared to assuming constant monthly emissions. Over the same region, including seasonality in agricultural waste burning results in a 2-3% higher total BC burden during spring. This is a relatively small increase, but agricultural waste burning contributes only around 6% to total BC emissions north of 40°N on an annual basis. Another potentially important factor is missing or underestimated emission sources. A recent study by Huang et al. (2015) estimate total anthropogenic BC emissions in Russia of 224 Gg, about 40% higher than in the ECLIPSEv4 inventory. Replacing the Russian BC emissions in the ECLIPSEv4 inventory with those from Huang et al. (2015) increases the modeled BC burden north of 65N by about 16% during fall, winter and early spring and 2-10% during summer. Another possibly underestimated emission source is open waste burning. Wiedinmyer et al. (2014) estimate that 631 Gg BC is emitted globally from open waste burning, nearly a factor 7 more than in the ECLIPSEv4 inventory. Moreover, they suggest that open waste burning may contribute 30-50% to total anthropogenic PM_{10} emissions in Russia, from where the near-surface transport of BC to the Arctic is effective (Stohl, 2006). Underestimation of this emission source may thus contribute to the too low modeled Arctic BC concentrations.

Eckhardt et al. (2015) show that models, including the OsloCTM2, have similar difficulties capturing the sulfate seasonality in the Arctic as they have for BC. At Zeppelin, the OsloCTM2-M7 underestimates also sulfur dioxide during spring, but overestimates concentrations during summer.

Figure 3 shows the seasonal cycle of CO for the same stations as in Fig. 2. In the Northern Hemisphere, the model captures the measured concentrations during summer, but

Atmos. Chem. Phys. Discuss., doi:10.5194/acp-2016-782, 2016
Manuscript under review for journal Atmos. Chem. Phys.
Published: 9 September 2016

Atmospheric Chemistry and Physics Discussions

underestimates the magnitude during winter/spring, a feature that has been shown also for other models in previous studies (Emmons et al., 2015; Monks et al., 2015). We also compare results at additional Southern Hemisphere locations (not shown here). In the Southern Hemisphere, the model generally reproduces the magnitude better, with a slight overestimation during winter/spring at several stations. The ability of the model to reproduce the seasonal cycle and magnitude of CO, in particular at remote Southern Hemispheric stations that are mainly influenced by long-range transport, suggests that the model represents atmospheric transport reasonably well and points to other processes as the dominant source of uncertainty in the model.

FIGURE 3

3.1.2 Vertical profiles

Figures 4 and 5 show modeled vertical BC and CO profiles against measurements from six aircraft campaigns. Compared to measurements from ARCPAC and ARCTAS spring the OsloCTM2-M7 underestimates the magnitude of BC concentrations throughout the atmosphere (Fig. 4 (p),(r); MNB -0.8). During both these campaigns, air masses were heavily influence by biomass burning plumes, which are often not captured by global models. The same springtime discrepancy was also seen in the surface concentrations. However, the shape of the profile is reproduced reasonably well. The agreement is better for ARCTAS summer (Fig. 4 (q); MNB 0.05), but the model underestimates near-surface concentrations. The model also underestimates the magnitude of CO concentrations during these two campaigns (Fig. 5 (p-r)), but again captures the profile shape reasonably well, providing further indication of too low emissions as an important source of the discrepancy.

Measurements from HIPPO are separated into five latitude bands (Fig. 4 (a-o), Fig. 5 (a-o)). For most latitude bands and flights, there is reasonable agreement close to the surface. In the 60-80N latitude band, the model overestimates concentrations close to the surface during HIPPO1 and 2, but underestimates concentrations during HIPPO3. HIPPO3 was undertaken during spring and a similar underestimation was also seen in the modeled surface measurements at Barrow during this time of year (Fig. 2). The model typically fail to reproduce the layered structure of the measured vertical profiles. In particular the high-altitude concentrations in tropics and the southern mid-latitudes are overestimated. It should be noted that there are substantial differences between the three HIPPO campaigns although they all cover the Pacific. A better model-measurement agreement is found for HIPPO3 than for HIPPO1 and 2 (MNB

Atmos. Chem. Phys. Discuss., doi:10.5194/acp-2016-782, 2016
Manuscript under review for journal Atmos. Chem. Phys.
Published: 9 September 2016

1.1, 3.3 and 2.8, respectively). In contrast to BC, both the magnitude and shape of most vertical CO profiles compare well across all latitude bands

There is quite good agreement between measured and modeled BC and CO during the A-FORCE campaign (Fig. 4 (s), Fig. 5 (s); MNB -0.1), with model results falling within one standard deviation of the measured profile. The A-FORCE campaign was carried out downstream of nearby emission sources and the good agreement with observations suggests reasonable representation in the model of both emission magnitude in the region and the mixing with the free troposphere on timescales of a few days. On these temporal and spatial scales, the loss processes are of less importance for the aerosol distribution. In contrast, the HIPPO campaigns sampled older air masses and loss processes are more important.

Our overall findings are in line with other recent studies. The tendency to overestimate high altitude BC concentrations over the Pacific has been noted for several other model (Kipling et al., 2013; Samset et al., 2014; Schwarz et al., 2013; Wang et al., 2014). The vertical profiles from OsloCTM2-M7 also fall roughly within the range of the AeroCom Phase II models (Samset et al., 2014).

FIGURE 4

FIGURE 5

3.1.3 BC in snow

The OsloCTM2-M7 underestimates BC concentrations in snow compared to measurements, in particular in Russia, Svalbard and the Canadian Arctic. Here we find somewhat higher modeled concentrations than in previous studies (Lund & Berntsen, 2012; Skeie et al., 2011) owing to the updated emission inventory and shorter model time step for precipitation. However, this increase is not sufficient to fully compensate for the existing underestimation. The model and measurements agree better for many of the snow samples taken in China.

Towards late spring, the modeled concentrations are occasionally very high compared to the measurement, especially in Tromsø and the Arctic Ocean. This feature was also shown by Skeie et al. (2011). During melting, the model assumes that all BC accumulates at the surface. Observational evidence suggest this assumption may lead to an overestimation. For instance, scavenging fractions of 10-30% due to percolation of meltwater were found by Doherty et al. (2013) from measurements made in Alaska, Greenland and Norway during melt season.

Atmos. Chem. Phys. Discuss., doi:10.5194/acp-2016-782, 2016
Manuscript under review for journal Atmos. Chem. Phys.
Published: 9 September 2016

Atmospheric Chemistry and Physics Discussions

409

410 *3.2 Sensitivity of BC concentrations to changes in aging and scavenging*

411 This section discusses the sensitivity of modeled BC concentrations to the changes in aging and
412 scavenging processes in our experiments.

413 Table 2 summarizes the global BC burden and lifetime in each experiment. The global mean
414 burden (lifetime) is 133 Gg (6 days) in the base simulation, while there is considerable range
415 from 81 Gg (3.6 days) to about 185 Gg (8 days) across the experiments. This range still falls
416 within that of BC lifetimes from global models (e.g., Samset et al. (2014)).

417 TABLE 2

418 The largest changes in BC concentrations in the sensitivity experiments occur in remote regions
419 and we find only small differences in the model-measurement comparison at the more
420 urban/rural stations in Fig. 2. In the following we therefore focus on the Arctic stations (Alert,
421 Barrow, Pallas and Zeppelin), as well as the vertical profiles from the six aircraft campaigns.
422 Figure 6 shows seasonal Arctic surface concentrations compared to the measurements (left
423 column) and the absolute difference from the base in each experiment (right column). Figure 7
424 shows the vertical BC profiles for each campaign and experiment, compared to the baseline and
425 measurements.

426 FIGURE 6

427 FIGURE 7

428 A shorter atmospheric BC lifetime reduces the high-altitude overestimation at mid- and tropical
429 latitudes over the Pacific. This is in line with other recent studies, which have suggested that
430 the lifetime of BC in global models must be reduced in order for the models to reproduce the
431 HIPPO data (Hodnebrog et al., 2014; Samset et al., 2014; Wang et al., 2014). Both allowing for
432 convective scavenging of hydrophobic BC (ConvBCi) and reducing the amount of soluble
433 material required for aging (CoatThick0.5) substantially reduces the MNB for the HIPPO
434 campaigns compared to the baseline (from approx. 3 to -0.3 and 1, respectively). For vertical
435 profiles in most latitude bands, the former experiment results in the lowest MNB of the two.
436 However, the model is very sensitive to the fraction of hydrophobic BC assumed to be available
437 for removal (here 100% or 20%), which is an uncertain parameter. Surface concentrations at
438 Alert, Zeppelin, and Pallas are also reproduced reasonably well in these experiments, although

Atmos. Chem. Phys. Discuss., doi:10.5194/acp-2016-782, 2016
Manuscript under review for journal Atmos. Chem. Phys.
Published: 9 September 2016

439 the springtime underestimation discussed above remains. In other parts of the Arctic however,
440 the model performance is exacerbated. More specifically, the MNB for the ARCTAS and
441 ARCPAC campaigns increases and the underestimation of surface concentration at Barrow is
442 larger compared to the baseline. Similar effects are also found in the 60°-70°S region (Fig. 7
443 (e), (j)). In addition to aging and scavenging, several other factors likely contribute to the too
444 low modeled Arctic concentrations, including uncertainties in emissions and model resolution.
445 A recently published study point to the importance of model resolution as a source of
446 uncertainty, suggesting that a kilometer-order resolution is required for more accurate
447 representation of BC concentrations in the Arctic (Sato et al., 2016).
448
449 Conversely, increasing the amount of soluble material required for aging increases the BC
450 lifetime. This in turn results in an increased potential for long-range transport and increase in
451 Arctic surface concentrations. However, with the exception of Barrow during spring, increasing
452 the number of required ML (CoatThick1.4, CoatThick2.3) does not result in marked
453 improvements in modeled Arctic surface concentrations compared to measurements. The
454 longer aging time in these experiments also results in a poorer agreement with the HIPPO
455 measurements, both close to the surface and at high altitudes. Moreover, even with the longer
456 lifetime and consequent increases in Arctic BC concentrations, the model does not reproduce
457 the vertical profiles from ARCTAS and ARCPAC. The experiments also result in reduced
458 concentrations of BC in snow in our model. In these cases, the aging time is longer and more
459 BC hence resides in the insoluble mode, unavailable for wet scavenging. Hence, in the
460 OsloCTM2-M7 a slower BC aging alone does not result in significant improvements in model-
461 measurement discrepancies.
462
463 Reducing the scavenging of BC by large-scale ice clouds and increasing the fraction of biomass
464 burning emissions initially in the accumulation mode, have only a minor influence on both
465 Arctic surface concentrations and modeled vertical profiles compared to the baseline. This is
466 also the case for the combined reduction in scavenging by large-scale ice clouds and increased
467 convective scavenging of hydrophobic aerosols.
468
469 In terms of BC concentrations in snow, smaller improvements are found, but none of the
470 experiments improve the model-measurement comparison of BC in snow simultaneously in all
471 regions.
472

Atmos. Chem. Phys. Discuss., doi:10.5194/acp-2016-782, 2016
Manuscript under review for journal Atmos. Chem. Phys.
Published: 9 September 2016

Measurements at mid-latitudes have shown that nitrate is frequently present in internal aerosol mixtures and contribute to the aging of BC (Pratt & Prather, 2010; Shiraiwa et al., 2007). The addition of nitric acid in the microphysical BC parameterization is a novel treatment in the CTM2-M7 and these experiments are discussed separately here. Allowing for nitric acid to condense on the aerosols results in a faster aging as more soluble material is available than when only sulfate is allowed to contribute and hence reduces the global BC lifetime. This in turn reduces high-altitude BC concentrations and leads to a better agreement with the HIPPO measurements (MNB between 0.4 and 0.7 for HIPPO1 and 2 in NitCondv2). Furthermore, BC snow concentrations across all regions except Greenland increase in this experiment, although not enough to fully account for the existing underestimation compared to measurements. However, the Arctic atmospheric BC concentrations are significantly reduced, resulting in a poorer model performance compared to both measured vertical profiles and surface concentrations in this region.

In this study, we have taken a first step towards inclusion of nitrate in the microphysical aerosol parameterization. This should however be studied further in future work. For instance the current setup only treats the condensation by nitric acid, not coagulation with nitrate aerosols. Furthermore, it is uncertain how effectively nitric acid increases the hygroscopicity of BC. Here we have assumed 5 ML. In two additional sensitivity tests we also investigate the impact of 1 and 10 ML and find substantial impacts on modeled BC concentrations. Existing model-measurement discrepancies in nitrate and sulfate concentrations also contribute to uncertainties.

In this work, we have not considered combinations of or regionally differing sensitivity experiments, for instance increased coating thickness required at high-latitudes in combination with more efficient removal by convective precipitation in low and mid-latitudes. Moreover, there are important details that are not captured in the OsloCTM2-M7. One example is related to the particle hydrophilicity/hygropscopicity. The OsloCTM2-M7 assumes that particles can automatically act as cloud condensation nuclei once they are transferred from the hydrophobic to hydrophilic mode. However, the cloud condensating activity of hydrophilic and hygroscopic particles also depends on the atmospheric supersaturation (Koehler et al., 2009; Petters & Kreidenweis, 2007). Furthermore, particles may not merely be hydrophilic or not as assumed by models, but rather exhibit a whole range of degrees of hydrophilicity. The ice nucleating efficiency of BC is also relatively poorly known. Our results underline the importance of more

Atmos. Chem. Phys. Discuss., doi:10.5194/acp-2016-782, 2016
Manuscript under review for journal Atmos. Chem. Phys.
Published: 9 September 2016

observations, in particular of the mixing state and scavenging of BC, as well as experimental data to improve process understanding.

3.3 Climate impacts

The changes in BC concentrations in our experiments can in turn affect the climate impact, especially when changes occur at altitudes where the efficacy of BC forcing and temperature response is strong. Changes in global radiative forcing (RF) and surface temperature (TS) from the baseline in each experiment are estimated using a kernel approach based on results from Samset and Myhre (2015) (see Sect. 2.4) and presented in Table 2.

Relative to the baseline, a decrease in global-mean BC ERFari (i.e., net of direct and semi-direct aerosol-radiation interactions) of -49 and -45 mW/m^2 is estimated for the two experiments that lead to the most marked improvements (i.e., strongest reduction in MNB) in vertical profiles compared to measurements over the Pacific (ConvBCi and NitCondv2). In these two experiments, allowing for convective removal of hydrophobic BC and adding condensation by gas-phase nitric acid reduces BC concentrations at high altitudes where the forcing efficacy is strong. Reducing the amount of sulfate required for BC aging also gives a notable decrease in ERFari of -26 mW/m^2. Changes in ERFari of similar magnitudes but opposite sign are estimated for the CoatThick1.4 and CoatThick2.3 experiments. The change in surface temperature response is also largest for three former experiments, resulting in a decrease of -25 mK compared to the baseline.

To place the impact of our experiments in context, we calculate the change in direct forcing only (i.e., RFari) and compare with existing best estimates of the total pre-industrial to present BC RFari. The Fifth IPCC Assessment Report reports a best estimate of RFari due to BC from all sources of 0.6 W/m^2 (Boucher et al., 2013), while Bond et al. (2013) give a slightly higher estimate of 0.71 W/m^2. Depending on experiment, the changes estimated here are on the order of 10 to 30% of the total BC RFari relative to pre-industrial.

Since our study also focuses on Arctic BC, we estimate the change in ERFari and TS caused by the changes in the BC profiles over this region. The resulting ERFari changes are generally larger than in the global-mean case. For all except two cases the Arctic TS changes are also larger than the global-mean changes. This partly reflects the large BC concentration changes in this region in our experiments and partly a smaller contribution of the semi-direct effect to the ERFari, which acts to offset less of the RFari than on global average. The Arctic surface

Atmos. Chem. Phys. Discuss., doi:10.5194/acp-2016-782, 2016
Manuscript under review for journal Atmos. Chem. Phys.
Published: 9 September 2016

temperature response to BC forcing exerted in the lower atmosphere, where a substantial impact on BC concentrations is seen in several of the experiments, is also stronger than in lower latitudes.

There is, however, an important caveat when using the temperature kernel from Samset and Myhre (2015) to estimate Arctic impacts. Because the BC perturbations at each altitude were applied uniformly in that model layer, the impact on temperature in a specific gridbox may be due both to forcing exerted locally and to remote forcing through large-scale circulation impacts. To exclude any influence of BC forcing exerted outside the Arctic region, we also use results from Flanner (2013) to estimate the TS changes. Using the same model as Samset and Myhre (2015), Flanner (2013) imposed BC perturbations at five different altitudes over the Arctic only, hence calculating the Arctic TS to only local effects. The resulting temperature kernel has previously been used to assess the impact of regional on-road diesel BC emissions (Lund et al., 2014). When used here to estimate the impact of our experiments, we find similar changes in Arctic TS to those estimated using results from Samset and Myhre (2015), with one notable exception. In three of the experiments (EmisTest, LSice12 and CombPert) the two different approaches produce changes in net Arctic TS of opposite sign. This is caused by slightly different efficacies in the two temperature kernels above 500 hPa altitude, where these experiments have their largest effect on BC concentrations. For most of the remaining experiments, using the temperature kernel from Samset and Myhre (2015) result in slightly stronger changes in net Arctic TS, reflecting the higher efficacy below 850 hPa compared to the Flanner (2013) kernel.

4 Summary and conclusions

We have performed a range of experiments to investigate the sensitivity of BC concentrations modeled by the OsloCTM2-M7 to parameters controlling the aerosol scavenging and aging and how these processes influence the existing model-measurement discrepancies, focusing simultaneously on Arctic surface concentrations and remote vertical distributions of BC. The experiments include a novel treatment of condensation of nitric acid on BC. Furthermore, the subsequent impact of concentration changes on radiative forcing and surface temperature response is estimated.

The OsloCTM2-M7 underestimates annual averaged BC surface concentrations, with a mean normalized bias (MNB) of -0.55. The model is better able to reproduce the observed seasonal

Atmos. Chem. Phys. Discuss., doi:10.5194/acp-2016-782, 2016
Manuscript under review for journal Atmos. Chem. Phys.
Published: 9 September 2016

variation and magnitude of Arctic BC surface concentrations compared to previous OsloCTM2 studies, but model-measurement discrepancies remain, particularly during spring. The OsloCTM2-M7 overestimates high-altitude BC concentrations over the Pacific compared to measurements from the HIPPO flight campaign, as has been found also for several other global models.

We find that a shorter atmospheric BC lifetime in the model reduces the high-altitude overestimation at mid- and tropical latitudes over the Pacific. This is in line with other recent studies which have suggested that the lifetime of BC in global models must be reduced in order for the models to reproduce the HIPPO data (Hodnebrog et al., 2014; Samset et al., 2014; Wang et al., 2014). Both allowing for convective scavenging of hydrophobic BC and reducing the amont of soluble material required for aging significantly improves (i.e., reduces the MNB) the comparison with vertical profiles from HIPPO compared to the baseline. In the case of convective scavenging, the model is sensitive to the fraction of hydrophobic BC assumed to be available for removal, a parameter with large associated uncertaines. While the surface concentrations at the Arctic stations of Alert, Zeppelin and Pallas remain in reasonable agreement with observations in the two former experiments, the comparison with measurements at Barrow and the ARCTAS and ARCPAC fligh campaigns becomes poorer. Conversely, changes in processes that lead to a longer BC lifetime excacerbates the high-altitude overestimation over the Pacific and result in an overestimation of Arctic surface concentrations during winter. Moreover, despite increases compared to the baseline, the BC concentration in snow and during flight campaigns in the Arctic is still underestimated.

Measurements at mid-latitudes have shown that nitrate is frequently present in internal aerosol mixtures and contribute to the aging of BC (Pratt & Prather, 2010; Shiraiwa et al., 2007). In this study, we have taken a first step towards including this process in the OsloCTM2-M7 by allowing for aging of BC by condensation of nitric acid. This results in a faster aging and hence a reduced global lifetime, which in turn reduces high-altitude BC concentrations and leads to a better agreement with the HIPPO measurements. Furthermore, BC snow concentrations across all regions except Greenland increase in this experiment, although not enough to eliminate the underestimation compared to measurements. However, the Arctic atmospheric BC concentrations are substantially reduced, resulting in a poorer model performance compared to both measured vertical profiles and surface concentrations in this region. A number of

603 uncertainties remain, including how effectively nitric acid increases the hygroscopicity of BC
604 and how coagulation with nitrate aerosols influence aging, and should be studies further.
605
606 Our experiments result in a non-negligible impact on radiative forcing (RF) and surface
607 temperature (TS). Compared to the baseline, decreases in the global RFari (i.e., direct RF) on
608 the order of 10-30% of the total pre-industrial to present BC direct forcing is estimated for the
609 experiments that result in the largest changes in BC concentrations. Notable decreases in both
610 ERFari (i.e., direct plus semi-direct RF) and TS is also estimated for the experiments which
611 leads to the most marked improvements (i.e., strongest reduction in MNB) in vertical BC
612 profiles compared to measurements over the Pacific.
613
614 While we find that globally tuning parameters related to aging and scavenging can improve the
615 representation of BC in the OsloCTM2-M7 compared to measurements in specific regions, our
616 results also show that such improvements can result from changes in several processes and
617 dependen on assumptions about uncertain parameters such as the ice nucleating efficacy of BC
618 and the change in hygroscopicity with aging. It is also important to be aware of potential
619 tradeoffs in model performance between different regions. Other important sources of
620 uncertainty, particularly for Arctic BC, such as model resolution has not been investigated here.
621 Our results underline the importance of more observations and experimental data to improve
622 process understanding and thus further constrain models.
623
624 **Acknowledgements**

625 This work was funded by the Research Council of Norway through the projects TEMPO,
626 SLAC and AC/BC. We also acknowledge the Reseach Council of Norway's programme for
627 supercomputing (NOTUR). We thank Professor Yutaka Kondo, University of Tokyo, for
628 providing results from the A-FORCE flight campaign.

629
630
631
632
633

634

635

636

637

638

639 **References:**

640 Amann M., Bertok I., Borken-Kleefeld J., Cofala J., Heyes C., Höglund-Isaksson L., Klimont Z., Nguyen
641 B., Posch M., Rafaj P., Sandler R., Schöpp W., Wagner F. & Winiwarter W. (2011). Cost-effective
642 control of air quality and greenhouse gases in Europe: Modeling and policy applications.
643 *Environmental Modelling & Software.* 26(12), 1489-1501, DOI:
644 http://dx.doi.org/10.1016/j.envsoft.2011.07.012.
645 AMAP (2015). AMAP Assessment 2015: Black carbon and ozone as Arctic climate forcers. Arctic
646 Monitoring and Assessment Programme (AMAP), Oslo, Norway.
647 Anenberg S. C., Schwartz J., Shindell D., Amann M., Faluvegi G., Klimont Z., Janssens-Maenhout G.,
648 Pozzoli L., Van Dingenen R., Vignati E., Emberson L., Muller N. Z., West J. J., Williams M., Demkine V.,
649 Hicks W. K., Kuylenstierna J., Raes F. & Ramanathan V. (2012). Global Air Quality and Health Co-
650 benefits of Mitigating Near-Term Climate Change through Methane and Black Carbon Emission
651 Controls. *Environmental Health Perspectives.* 120(6), 831-839, DOI: 10.1289/ehp.1104301.
652 Aunan K., Fang J., Hu T., Seip H. M. & Vennemo H. (2006). Climate Change and Air Quality—
653 Measures with Co-Benefits in China. *Environmental Science & Technology.* 40(16), 4822-4829, DOI:
654 10.1021/es062994k.
655 Balkanski Y., Myhre G., Gauss M., Raedel G., Highwood E. J. & Shine K. P. (2010). Direct radiative
656 effect of aerosols emitted by transport: from road, shipping and aviation. *Atmospheric Chemistry*
657 *and Physics.* 10(10), 4477-4489, DOI: 10.5194/acp-10-4477-2010.
658 Ban-Weiss G., Cao L., Bala G. & Caldeira K. (2011). Dependence of climate forcing and response on
659 the altitude of black carbon aerosols. *Climate Dynamics*, 1-15, DOI: 10.1007/s00382-011-1052-y.
660 Bauer S. E., Koch D., Unger N., Metzger S. M., Shindell D. T. & Streets D. G. (2007). Nitrate aerosols
661 today and in 2030: a global simulation including aerosols and tropospheric ozone. *Atmospheric*
662 *Chemistry and Physics.* 7(19), 5043-5059.
663 Bellouin N., Rae J., Jones A., Johnson C., Haywood J. & Boucher O. (2011). Aerosol forcing in the
664 Climate Model Intercomparison Project (CMIP5) simulations by HadGEM2-ES and the role of
665 ammonium nitrate. *Journal of Geophysical Research-Atmospheres.* 116, D20206, DOI:
666 10.1029/2011jd016074.
667 Berglen T. F., Berntsen T. K., Isaksen I. S. A. & Sundet J. K. (2004). A global model of the coupled
668 sulfur/oxidant chemistry in the troposphere: The sulfur cycle. *Journal of Geophysical Research-*
669 *Atmospheres.* 109(D19), D19310, DOI: 10.1029/2003jd003948.
670 Berntsen T., Fuglestvedt J., Myhre G., Stordal F. & Berglen T. F. (2006). Abatement of greenhouse
671 gases: Does location matter? *Climatic Change.* 74(4), 377-411, DOI: 10.1007/s10584-006-0433-4.
672 Bollasina M. A., Ming Y., Ramaswamy V., Schwarzkopf M. D. & Naik V. (2014). Contribution of local
673 and remote anthropogenic aerosols to the twentieth century weakening of the South Asian
674 Monsoon. *Geophysical Research Letters.* 41(2), 680-687, DOI: 10.1002/2013GL058183.
675 Bond T. C. & Bergstrom R. W. (2006). Light absorption by carbonaceous particles: An investigative
676 review. *Aerosol Science and Technology.* 40(1), 27-67, DOI: 10.1080/02786820500421521.

677 Bond T. C., Doherty S. J., Fahey D. W., Forster P. M., Berntsen T., DeAngelo B. J., Flanner M. G., Ghan
678 S., Kärcher B., Koch D., Kinne S., Kondo Y., Quinn P. K., Sarofim M. C., Schultz M. G., Schulz M.,
679 Venkataraman C., Zhang H., Zhang S., Bellouin N., Guttikunda S. K., Hopke P. K., Jacobson M. Z.,
680 Kaiser J. W., Klimont Z., Lohmann U., Schwarz J. P., Shindell D., Storelvmo T., Warren S. G. & Zender
681 C. S. (2013). Bounding the role of black carbon in the climate system: A scientific assessment.
682 *Journal of Geophysical Research: Atmospheres.* 118(11), 5380-5552, DOI: 10.1002/jgrd.50171.
683 Boucher O., Randall D., Artaxo P., Bretherton C., Feingold G., Forster P., Kerminen V.-M., Kondo Y.,
684 Liao H., Lohmann U., Rasch P., Satheesh S. K., Sherwood S., Stevens B. & Zhang X. Y. (2013). Clouds
685 and Aerosols. In: Climate Change 2013: The Physical Science Basis. Contribution of Working Group I
686 to the Fifth Assessment Report of the Intergovernmental Panel on Climate Change [Stocker, T.F., D.
687 Qin, G.-K. Plattner, M. Tignor, S.K. Allen, J. Boschung, A. Nauels, Y. Xia, V. Bex and P.M. Midgley
688 (eds.)]. Cambridge University Press, Cambridge, United Kingdom and New York, NY, USA.
689 Bourgeois Q. & Bey I. (2011). Pollution transport efficiency toward the Arctic: Sensitivity to aerosol
690 scavenging and source regions. *Journal of Geophysical Research: Atmospheres.* 116(D8), n/a-n/a,
691 DOI: 10.1029/2010JD015096.
692 Bowerman N. H. A., Frame D. J., Huntingford C., Lowe J. A., Smith S. M. & Allen M. R. (2013). The role
693 of short-lived climate pollutants in meeting temperature goals. *Nature Clim. Change.* 3(12), 1021-
694 1024, DOI: 10.1038/nclimate2034.
695 Breider T. J., Mickley L. J., Jacob D. J., Wang Q., Fisher J. A., Chang R. Y. W. & Alexander B. (2014).
696 Annual distributions and sources of Arctic aerosol components, aerosol optical depth, and aerosol
697 absorption. *Journal of Geophysical Research: Atmospheres.* 119(7), 4107-4124, DOI:
698 10.1002/2013JD020996.
699 Brock C. A., Cozic J., Bahreini R., Froyd K. D., Middlebrook A. M., McComiskey A., Brioude J., Cooper
700 O. R., Stohl A., Aikin K. C., de Gouw J. A., Fahey D. W., Ferrare R. A., Gao R. S., Gore W., Holloway J. S.,
701 Hübler G., Jefferson A., Lack D. A., Lance S., Moore R. H., Murphy D. M., Nenes A., Novelli P. C.,
702 Nowak J. B., Ogren J. A., Peischl J., Pierce R. B., Pilewskie P., Quinn P. K., Ryerson T. B., Schmidt K. S.,
703 Schwarz J. P., Sodemann H., Spackman J. R., Stark H., Thomson D. S., Thornberry T., Veres P., Watts L.
704 A., Warneke C. & Wollny A. G. (2011). Characteristics, sources, and transport of aerosols measured
705 in spring 2008 during the aerosol, radiation, and cloud processes affecting Arctic Climate (ARCPAC)
706 Project. *Atmos. Chem. Phys.* 11(6), 2423-2453, DOI: 10.5194/acp-11-2423-2011.
707 Browse J., Carslaw K. S., Arnold S. R., Pringle K. & Boucher O. (2012). The scavenging processes
708 controlling the seasonal cycle in Arctic sulphate and black carbon aerosol. *Atmospheric Chemistry*
709 *and Physics.* 12(15), 6775-6798, DOI: 10.5194/acp-12-6775-2012.
710 Cozic J., Verheggen B., Mertes S., Connolly P., Bower K., Petzold A., Baltensperger U. & Weingartner
711 E. (2007). Scavenging of black carbon in mixed phase clouds at the high alpine site Jungfraujoch.
712 *Atmospheric Chemistry and Physics.* 7(7), 1797-1807.
713 Doherty S. J., Warren S. G., Grenfell T. C., Clarke A. D. & Brandt R. E. (2010). Light-absorbing
714 impurities in Arctic snow. *Atmospheric Chemistry and Physics.* 10, 11647-11680.
715 Doherty S. J., Grenfell T. C., Forsstrom S., Hegg D. L., Brandt R. E. & Warren S. G. (2013). Observed
716 vertical redistribution of black carbon and other insoluble light-absorbing particles in melting snow.
717 *Journal of Geophysical Research-Atmospheres.* 118(11), 5553-5569, DOI: 10.1002/jgrd.50235.
718 Eckhardt S., Quennehen B., Olivié D. J. L., Berntsen T. K., Cherian R., Christensen J. H., Collins W.,
719 Crepinsek S., Daskalakis N., Flanner M., Herber A., Heyes C., Hodnebrog Ø., Huang L., Kanakidou M.,
720 Klimont Z., Langner J., Law K. S., Lund M. T., Mahmood R., Massling A., Myriokefalitakis S., Nielsen I.
721 E., Nøjgaard J. K., Quaas J., Quinn P. K., Raut J. C., Rumbold S. T., Schulz M., Sharma S., Skeie R. B.,
722 Skov H., Uttal T., von Salzen K. & Stohl A. (2015). Current model capabilities for simulating black
723 carbon and sulfate concentrations in the Arctic atmosphere: a multi-model evaluation using a
724 comprehensive measurement data set. *Atmos. Chem. Phys.* 15(16), 9413-9433, DOI: 10.5194/acp-
725 15-9413-2015.
726 Ekman A. M. L., Wang C., Strom J. & Krejci R. (2006). Explicit simulation of aerosol physics in a cloud-
727 resolving model: Aerosol transport and processing in the free troposphere. *J. Atmos. Sci.* 63(2), 682-
728 696, DOI: 10.1175/jas3645.1.

729 Emmons L. K., Arnold S. R., Monks S. A., Huijnen V., Tilmes S., Law K. S., Thomas J. L., Raut J. C.,
730 Bouarar I., Turquety S., Long Y., Duncan B., Steenrod S., Strode S., Flemming J., Mao J., Langner J.,
731 Thompson A. M., Tarasick D., Apel E. C., Blake D. R., Cohen R. C., Dibb J., Diskin G. S., Fried A., Hall S.
732 R., Huey L. G., Weinheimer A. J., Wisthaler A., Mikoviny T., Nowak J., Peischl J., Roberts J. M., Ryerson
733 T., Warneke C. & Helmig D. (2015). The POLARCAT Model Intercomparison Project (POLMIP):
734 overview and evaluation with observations. *Atmos. Chem. Phys.* 15(12), 6721-6744, DOI:
735 10.5194/acp-15-6721-2015.
736 EPA (2012). Report to Congress on black carbon. US Environmental Protection Agency, Washington
737 DC, USA.
738 Fan S. M., Schwarz J. P., Liu J., Fahey D. W., Ginoux P., Horowitz L. W., Levy H., Ming Y. & Spackman J.
739 R. (2012). Inferring ice formation processes from global-scale black carbon profiles observed in the
740 remote atmosphere and model simulations. *Journal of Geophysical Research: Atmospheres.*
741 117(D23), n/a-n/a, DOI: 10.1029/2012JD018126.
742 Flanner M. G., Zender C. S., Hess P. G., Mahowald N. M., Painter T. H., Ramanathan V. & Rasch P. J.
743 (2009). Springtime warming and reduced snow cover from carbonaceous particles. *Atmospheric*
744 *Chemistry and Physics.* 9(7), 2481-2497.
745 Flanner M. G. (2013). Arctic climate sensitivity to local black carbon. *Journal of Geophysical*
746 *Research-Atmospheres.* 118(4), 1840-1851, DOI: 10.1002/jgrd.50176.
747 Fujino J., Nair R., Kainuma M., Masui T. & Matsuoka Y. (2006). Multi-gas mitigation analysis on
748 stabilization scenarios using AIM global model. *Energy Journal.* Special issue: 3, 343-353.
749 Grieshop A. P., Reynolds C. C. O., Kandlikar M. & Dowlatabadi H. (2009). A black-carbon mitigation
750 wedge. *Nature Geoscience.* 2(8), 533-534, DOI: 10.1038/ngeo595.
751 Grini A. (2007), Including the M7 aerosol dynamics model in the global Chemistry Transport Model
752 Oslo CTM2, Report no 133; ISBN 82-91885-37-0.
753 Hijioka J., Matsuoka Y., Nishimoto H., Masui M. & Kainuma M. (2008). Global GHG emissions
754 scenarios under GHG concentration stabilization targets. *Journal of Global Environmental*
755 *Engineering.* 13, 97-108.
756 Hodnebrog Ø., Myhre G. & Samset B. H. (2014). How shorter black carbon lifetime alters its climate
757 effect. *Nat Commun.* 5, DOI: 10.1038/ncomms6065.
758 Hoose C., Kristjansson J. E., Chen J. P. & Hazra A. (2010). A Classical-Theory-Based Parameterization
759 of Heterogeneous Ice Nucleation by Mineral Dust, Soot, and Biological Particles in a Global Climate
760 Model. *J. Atmos. Sci.* 67(8), 2483-2503, DOI: 10.1175/2010jas3425.1.
761 Huang K., Fu J. S., Prikhodko V. Y., Storey J. M., Romanov A., Hodson E. L., Cresko J., Morozova I.,
762 Ignatieva Y. & Cabaniss J. (2015). Russian anthropogenic black carbon: Emission reconstruction and
763 Arctic black carbon simulation. *Journal of Geophysical Research: Atmospheres.* 120(21), 11,306-
764 311,333, DOI: 10.1002/2015JD023358.
765 Jacob D. J., Crawford J. H., Maring H., Clarke A. D., Dibb J. E., Emmons L. K., Ferrare R. A., Hostetler C.
766 A., Russell P. B., Singh H. B., Thompson A. M., Shaw G. E., McCauley E., Pederson J. R. & Fisher J. A.
767 (2010). The Arctic Research of the Composition of the Troposphere from Aircraft and Satellites
768 (ARCTAS) mission: design, execution, and first results. *Atmos. Chem. Phys.* 10(11), 5191-5212, DOI:
769 10.5194/acp-10-5191-2010.
770 Kajino M., Inomata Y., Sato K., Ueda H., Han Z., An J., Katata G., Deushi M., Maki T., Oshima N.,
771 Kurokawa J., Ohara T., Takami A. & Hatakeyama S. (2012). Development of the RAQM2 aerosol
772 chemical transport model and predictions of the Northeast Asian aerosol mass, size, chemistry, and
773 mixing type. *Atmospheric Chemistry and Physics.* 12(24), 11833-11856, DOI: 10.5194/acp-12-11833-
774 2012.
775 Kipling Z., Stier P., Schwarz J. P., Perring A. E., Spackman J. R., Mann G. W., Johnson C. E. & Telford P.
776 J. (2013). Constraints on aerosol processes in climate models from vertically-resolved aircraft
777 observations of black carbon. *Atmos. Chem. Phys.* 13(12), 5969-5986, DOI: 10.5194/acp-13-5969-
778 2013.
779 Kipling Z., Stier P., Johnson C. E., Mann G. W., Bellouin N., Bauer S. E., Bergman T., Chin M., Diehl T.,
780 Ghan S. J., Iversen T., Kirkevåg A., Kokkola H., Liu X., Luo G., van Noije T., Pringle K. J., von Salzen K.,

781 Schulz M., Seland Ø., Skeie R. B., Takemura T., Tsigaridis K. & Zhang K. (2016). What controls the
782 vertical distribution of aerosol? Relationships between process sensitivity in HadGEM3–UKCA and
783 inter-model variation from AeroCom Phase II. *Atmos. Chem. Phys.* 16(4), 2221-2241, DOI:
784 10.5194/acp-16-2221-2016.
785 Klimont Z., Cofala J., Xing J., Wei W., Zhang C., Wang S., Kejun J., Bhandari P., Mathur R., Purohit P.,
786 Rafaj P., Chambers A., Amann M. & Hao J. (2009). Projections of SO2, NOx and carbonaceous
787 aerosols emissions in Asia. *Tellus B.* 61(4), 602-617, DOI: 10.1111/j.1600-0889.2009.00428.x.
788 Klimont Z., Kupiainen K., Heyes C., Purohit P., Cofala J., Rafaj P., Schoepp W. & Borken-Kleefeld J.
789 (2016). Global anthropogenic emissions of particulate matter including black carbon. In preparation.
790 Koch D., Menon S., Del Genio A., Ruedy R., Alienov I. & Schmidt G. A. (2009a). Distinguishing Aerosol
791 Impacts on Climate over the Past Century. *Journal of Climate.* 22(10), 2659-2677, DOI:
792 10.1175/2008jcli2573.1.
793 Koch D., Schulz M., Kinne S., McNaughton C., Spackman J. R., Balkanski Y., Bauer S., Berntsen T., Bond
794 T. C., Boucher O., Chin M., Clarke A., De Luca N., Dentener F., Diehl T., Dubovik O., Easter R., Fahey D.
795 W., Feichter J., Fillmore D., Freitag S., Ghan S., Ginoux P., Gong S., Horowitz L., Iversen T., Kirkevag A.,
796 Klimont Z., Kondo Y., Krol M., Liu X., Miller R., Montanaro V., Moteki N., Myhre G., Penner J. E.,
797 Perlwitz J., Pitari G., Reddy S., Sahu L., Sakamoto H., Schuster G., Schwarz J. P., Seland O., Stier P.,
798 Takegawa N., Takemura T., Textor C., van Aardenne J. A. & Zhao Y. (2009b). Evaluation of black
799 carbon estimations in global aerosol models. *Atmospheric Chemistry and Physics.* 9(22), 9001-9026,
800 DOI: 10.5194/acp-9-9001-2009.
801 Koch D. & Del Genio A. D. (2010). Black carbon semi-direct effects on cloud cover: review and
802 synthesis. *Atmospheric Chemistry and Physics.* 10(16), 7685-7696, DOI: 10.5194/acp-10-7685-2010.
803 Koehler K. A., DeMott P. J., Kreidenweis S. M., Popovicheva O. B., Petters M. D., Carrico C. M., Kireeva
804 E. D., Khokhlova T. D. & Shonija N. K. (2009). Cloud condensation nuclei and ice nucleation activity of
805 hydrophobic and hydrophilic soot particles. *Physical Chemistry Chemical Physics.* 11(36), 7906-7920,
806 DOI: 10.1039/b905334b.
807 Kopp R. E. & Mauzerall D. L. (2010). Assessing the climatic benefits of black carbon mitigation.
808 *Proceedings of the National Academy of Sciences of the United States of America.* 107(26), 11703-
809 11708, DOI: 10.1073/pnas.0909605107.
810 Lee Y. H., Lamarque J. F., Flanner M. G., Jiao C., Shindell D. T., Berntsen T., Bisiaux M. M., Cao J.,
811 Collins W. J., Curran M., Edwards R., Faluvegi G., Ghan S., Horowitz L. W., McConnell J. R., Ming J.,
812 Myhre G., Nagashima T., Naik V., Rumbold S. T., Skeie R. B., Sudo K., Takemura T., Thevenon F., Xu B.
813 & Yoon J. H. (2013). Evaluation of preindustrial to present-day black carbon and its albedo forcing
814 from Atmospheric Chemistry and Climate Model Intercomparison Project (ACCMIP). *Atmospheric*
815 *Chemistry and Physics.* 13(5), 2607-2634, DOI: 10.5194/acp-13-2607-2013.
816 Liu J., Fan S., Horowitz L. W. & Levy H., II (2011). Evaluation of factors controlling long-range
817 transport of black carbon to the Arctic. *Journal of Geophysical Research-Atmospheres.* 116, D04307,
818 DOI: 10.1029/2010jd015145.
819 Lohmann U. & Feichter J. (2005). Global indirect aerosol effects: a review. *Atmos. Chem. Phys.* 5(3),
820 715-737, DOI: 10.5194/acp-5-715-2005.
821 Lund M. T. & Berntsen T. (2012). Parameterization of black carbon aging in the OsloCTM2 and
822 implications for regional transport to the Arctic. *Atmos. Chem. Phys.* 12(15), 6999-7014, DOI:
823 10.5194/acp-12-6999-2012.
824 Lund M. T., Berntsen T. K., Heyes C., Klimont Z. & Samset B. H. (2014). Global and regional climate
825 impacts of black carbon and co-emitted species from the on-road diesel sector. *Atmospheric*
826 *Environment.* 98, 50-58, DOI: http://dx.doi.org/10.1016/j.atmosenv.2014.08.033.
827 Makkonen R., Romakkaniemi S., Kokkola H., Stier P., Raisanen P., Rast S., Feichter J., Kulmala M. &
828 Laaksonen A. (2012). Brightening of the global cloud field by nitric acid and the associated radiative
829 forcing. *Atmospheric Chemistry and Physics.* 12(16), 7625-7633, DOI: 10.5194/acp-12-7625-2012.
830 Metzger S., Dentener F., Krol M., Jeuken A. & Lelieveld J. (2002a). Gas/aerosol partitioning - 2. Global
831 modeling results. *Journal of Geophysical Research-Atmospheres.* 107(D16), 4313, DOI:
832 10.1029/2001jd001103.

833 Metzger S., Dentener F., Pandis S. & Lelieveld J. (2002b). Gas/aerosol partitioning: 1. A
834 computationally efficient model. *Journal of Geophysical Research-Atmospheres.* 107(D16), 4312,
835 DOI: 10.1029/2001jd001102.
836 Monks S. A., Arnold S. R., Emmons L. K., Law K. S., Turquety S., Duncan B. N., Flemming J., Huijnen V.,
837 Tilmes S., Langner J., Mao J., Long Y., Thomas J. L., Steenrod S. D., Raut J. C., Wilson C., Chipperfield
838 M. P., Diskin G. S., Weinheimer A., Schlager H. & Ancellet G. (2015). Multi-model study of chemical
839 and physical controls on transport of anthropogenic and biomass burning pollution to the Arctic.
840 *Atmos. Chem. Phys.* 15(6), 3575-3603, DOI: 10.5194/acp-15-3575-2015.
841 Myhre G., Grini A. & Metzger S. (2006). Modelling of nitrate and ammonium-containing aerosols in
842 presence of sea salt. *Atmos. Chem. Phys.* 6, 4809-4821.
843 Myhre G., Samset B. H., Schulz M., Balkanski Y., Bauer S., Berntsen T. K., Bian H., Bellouin N., Chin M.,
844 Diehl T., Easter R. C., Feichter J., Ghan S. J., Hauglustaine D., Iversen T., Kinne S., Kirkevag A.,
845 Lamarque J. F., Lin G., Liu X., Lund M. T., Luo G., Ma X., van Noije T., Penner J. E., Rasch P. J., Ruiz A.,
846 Seland O., Skeie R. B., Stier P., Takemura T., Tsigaridis K., Wang P., Wang Z., Xu L., Yu H., Yu F., Yoon J.
847 H., Zhang K., Zhang H. & Zhou C. (2013). Radiative forcing of the direct aerosol effect from AeroCom
848 Phase II simulations. *Atmospheric Chemistry and Physics.* 13(4), 1853-1877, DOI: 10.5194/acp-13-
849 1853-2013.
850 Oshima N., Kondo Y., Moteki N., Takegawa N., Koike M., Kita K., Matsui H., Kajino M., Nakamura H.,
851 Jung J. S. & Kim Y. J. (2012). Wet removal of black carbon in Asian outflow: Aerosol Radiative Forcing
852 in East Asia (A-FORCE) aircraft campaign. *Journal of Geophysical Research-Atmospheres.* 117,
853 D03204, DOI: 10.1029/2011jd016552.
854 Park R. J., Jacob D. J., Palmer P. I., Clarke A. D., Weber R. J., Zondlo M. A., Eisele F. L., Bandy A. R.,
855 Thornton D. C., Sachse G. W. & Bond T. C. (2005). Export efficiency of black carbon aerosol in
856 continental outflow: Global implications. *Journal of Geophysical Research-Atmospheres.* 110(D11),
857 D11205, DOI: 10.1029/2004jd005432.
858 Petters M. D. & Kreidenweis S. M. (2007). A single parameter representation of hygroscopic growth
859 and cloud condensation nucleus activity. *Atmospheric Chemistry and Physics.* 7(8), 1961-1971.
860 Petzold A., Ogren J. A., Fiebig M., Laj P., Li S. M., Baltensperger U., Holzer-Popp T., Kinne S.,
861 Pappalardo G., Sugimoto N., Wehrli C., Wiedensohler A. & Zhang X. Y. (2013). Recommendations for
862 reporting "black carbon" measurements. *Atmos. Chem. Phys.* 13(16), 8365-8379, DOI: 10.5194/acp-
863 13-8365-2013.
864 Popovicheva O. B., Persiantseva N. M., Tishkova V., Shonija N. K. & Zubareva N. A. (2008).
865 Quantification of water uptake by soot particles. *Environmental Research Letters.* 3(2), 025009, DOI:
866 10.1088/1748-9326/3/2/025009.
867 Popovicheva O. B., Persiantseva N. M., Kireeva E. D., Khokhlova T. D. & Shonija N. K. (2011).
868 Quantification of the Hygroscopic Effect of Soot Aging in the Atmosphere: Laboratory Simulations.
869 *Journal of Physical Chemistry A.* 115(3), 298-306, DOI: 10.1021/jp109238x.
870 Pratt K. A. & Prather K. A. (2010). Aircraft measurements of vertical profiles of aerosol mixing states.
871 *Journal of Geophysical Research-Atmospheres.* 115, D11305, DOI: 10.1029/2009jd013150.
872 Pringle K. J., Tost H., Message S., Steil B., Giannadaki D., Nenes A., Fountoukis C., Stier P., Vignati E. &
873 Leieved J. (2010). Description and evaluation of GMXe: a new aerosol submodel for global
874 simulations (v1). *Geoscientific Model Development.* 3(2), 391-412, DOI: 10.5194/gmd-3-391-2010.
875 Samset B. H. & Myhre G. (2011). Vertical dependence of black carbon, sulphate and biomass burning
876 aerosol radiative forcing. *Geophys. Res. Lett.* . 38, L24802, DOI: doi:10.1029/2011GL049697.
877 Samset B. H., Myhre G., Herber A., Kondo Y., Li S. M., Moteki N., Koike M., Oshima N., Schwarz J. P.,
878 Balkanski Y., Bauer S. E., Bellouin N., Berntsen T. K., Bian H., Chin M., Diehl T., Easter R. C., Ghan S. J.,
879 Iversen T., Kirkevåg A., Lamarque J. F., Lin G., Liu X., Penner J. E., Schulz M., Seland Ø., Skeie R. B.,
880 Stier P., Takemura T., Tsigaridis K. & Zhang K. (2014). Modelled black carbon radiative forcing and
881 atmospheric lifetime in AeroCom Phase II constrained by aircraft observations. *Atmos. Chem. Phys.*
882 14(22), 12465-12477, DOI: 10.5194/acp-14-12465-2014.

883 Samset B. H. & Myhre G. (2015). Climate response to externally mixed black carbon as a function of
884 altitude. *Journal of Geophysical Research: Atmospheres.* 120(7), 2913-2927, DOI:
885 10.1002/2014JD022849.
886 Sato Y., Miura H., Yashiro H., Goto D., Takemura T., Tomita H. & Nakajima T. (2016). Unrealistically
887 pristine air in the Arctic produced by current global scale models. *Scientific Reports.* 6, 26561, DOI:
888 10.1038/srep26561

889 http://www.nature.com/articles/srep26561#supplementary-information.
890 Schulz M., Textor C., Kinne S., Balkanski Y., Bauer S., Berntsen T., Berglen T., Boucher O., Dentener F.,
891 Guibert S., Isaksen I. S. A., Iversen T., Koch D., Kirkevag A., Liu X., Montanaro V., Myhre G., Penner J.
892 E., Pitari G., Reddy S., Seland O., Stier P. & Takemura T. (2006). Radiative forcing by aerosols as
893 derived from the AeroCom present-day and pre-industrial simulations. *Atmospheric Chemistry and*
894 *Physics.* 6, 5225-5246, DOI: 10.5194/acp-6-5225-2006.
895 Schwarz J. P., Gao R. S., Spackman J. R., Watts L. A., Thomson D. S., Fahey D. W., Ryerson T. B., Peischl
896 J., Holloway J. S., Trainer M., Frost G. J., Baynard T., Lack D. A., de Gouw J. A., Warneke C. & Del
897 Negro L. A. (2008). Measurement of the mixing state, mass, and optical size of individual black
898 carbon particles in urban and biomass burning emissions. *Geophysical Research Letters.* 35(13), DOI:
899 10.1029/2008gl033968.
900 Schwarz J. P., Samset B. H., Perring A. E., Spackman J. R., Gao R. S., Stier P., Schulz M., Moore F. L.,
901 Ray E. A. & Fahey D. W. (2013). Global-scale seasonally resolved black carbon vertical profiles over
902 the Pacific. *Geophysical Research Letters.* 40(20), 2013GL057775, DOI: 10.1002/2013GL057775.
903 Sharma S., Ishizawa M., Chan D., Lavoué D., Andrews E., Eleftheriadis K. & Maksyutov S. (2013). 16-
904 year simulation of Arctic black carbon: Transport, source contribution, and sensitivity analysis on
905 deposition. *Journal of Geophysical Research: Atmospheres.* 118(2), 943-964, DOI:
906 10.1029/2012JD017774.
907 Shindell D., Faluvegi G., Walsh M., Anenberg S. C., Van Dingenen R., Muller N. Z., Austin J., Koch D. &
908 Milly G. (2011). Climate, health, agricultural and economic impacts of tighter vehicle-emission
909 standards. *Nature Climate Change.* 1(1), 59-66, DOI: 10.1038/nclimate1066.
910 Shindell D. T., Chin M., Dentener F., Doherty R. M., Faluvegi G., Fiore A. M., Hess P., Koch D. M.,
911 MacKenzie I. A., Sanderson M. G., Schultz M. G., Schulz M., Stevenson D. S., Teich H., Textor C., Wild
912 O., Bergmann D. J., Bey I., Bian H., Cuvelier C., Duncan B. N., Folberth G., Horowitz L. W., Jonson J.,
913 Kaminski J. W., Marmer E., Park R., Pringle K. J., Schroeder S., Szopa S., Takemura T., Zeng G., Keating
914 T. J. & Zuber A. (2008). A multi-model assessment of pollution transport to the Arctic. *Atmospheric*
915 *Chemistry and Physics.* 8(17), 5353-5372, DOI: 10.5194/acp-8-5353-2008,.
916 Shindell D. T., Lamarque J. F., Schulz M., Flanner M., Jiao C., Chin M., Young P. J., Lee Y. H., Rotstayn
917 L., Mahowald N., Milly G., Faluvegi G., Balkanski Y., Collins W. J., Conley A. J., Dalsoren S., Easter R.,
918 Ghan S., Horowitz L., Liu X., Myhre G., Nagashima T., Naik V., Rumbold S. T., Skeie R., Sudo K., Szopa
919 S., Takemura T., Voulgarakis A., Yoon J. H. & Lo F. (2013). Radiative forcing in the ACCMIP historical
920 and future climate simulations. *Atmospheric Chemistry and Physics.* 13(6), 2939-2974, DOI:
921 10.5194/acp-13-2939-2013.
922 Shiraiwa M., Kondo Y., Moteki N., Takegawa N., Miyazaki Y. & Blake D. R. (2007). Evolution of mixing
923 state of black carbon in polluted air from Tokyo. *Geophysical Research Letters.* 34(16), L16803, DOI:
924 10.1029/2007gl029819.
925 Skeie R. B., Berntsen T., Myhre G., Pedersen C. A., Ström J., Gerland S. & Ogren J. A. (2011). Black
926 carbon in the atmosphere and snow, from pre-industrial times until present. *Atmospheric Chemistry*
927 *and Physics.* 11(14), 6809-6836, DOI: 10.5194/acp-11-6809-2011.
928 Sovde O. A., Gauss M., Smyshlyaev S. P. & Isaksen I. S. A. (2008). Evaluation of the chemical transport
929 model Oslo CTM2 with focus on arctic winter ozone depletion. *Journal of Geophysical Research-*
930 *Atmospheres.* 113(D9), D09304, DOI: 10.1029/2007jd009240.
931 Stohl A. (2006). Characteristics of atmospheric transport into the Arctic troposphere. *Journal of*
932 *Geophysical Research-Atmospheres.* 111(D11), D11306, DOI: 10.1029/2005jd006888.

933 Stohl A., Klimont Z., Eckhardt S., Kupiainen K., Shevchenko V. P., Kopeikin V. M. & Novigatsky A. N.
934 (2013). Black carbon in the Arctic: the underestimated role of gas flaring and residential combustion
935 emissions. *Atmos. Chem. Phys.* 13(17), 8833-8855, DOI: 10.5194/acp-13-8833-2013.
936 Streets D. G., Bond T. C., Carmichael G. R., Fernandes S. D., Fu Q., He D., Klimont Z., Nelson S. M., Tsai
937 N. Y., Wang M. Q., Woo J.-H. & Yarber K. F. (2003). An inventory of gaseous and primary aerosol
938 emissions in Asia in the year 2000. *Journal of Geophysical Research.* 108(D21), DOI:
939 10.1029/2002JD003093.
940 Textor C., Schulz M., Guibert S., Kinne S., Balkanski Y., Bauer S., Berntsen T., Berglen T., Boucher O.,
941 Chin M., Dentener F., Diehl T., Feichter J., Fillmore D., Ginoux P., Gong S., Grini A., Hendricks J.,
942 Horowitz L., Huang P., Isaksen I. S. A., Iversen T., Kloster S., Koch D., Kirkevag A., Kristjansson J. E.,
943 Krol M., Lauer A., Lamarque J. F., Liu X., Montanaro V., Myhre G., Penner J. E., Pitari G., Reddy M. S.,
944 Seland O., Stier P., Takemura T. & Tie X. (2007). The effect of harmonized emissions on aerosol
945 properties in global models - an AeroCom experiment. *Atmospheric Chemistry and Physics.* 7(17),
946 4489-4501.
947 UNEP/WMO (2011). Integrated assessment of black carbon and tropospheric ozone, 282 pp., United
948 Nations Environmental Programme, Nairobi, Kenya, and World Meteorological Organization, Geneva,
949 Switzerland.
950 van der Werf G. R., Randerson J. T., Giglio L., Collatz G. J., Mu M., Kasibhatla P. S., Morton D. C.,
951 DeFries R. S., Jin Y. & van Leeuwen T. T. (2010). Global fire emissions and the contribution of
952 deforestation, savanna, forest, agricultural, and peat fires (1997–2009). *Atmos. Chem. Phys.* 10(23),
953 11707-11735, DOI: 10.5194/acp-10-11707-2010.
954 Vignati E., Wilson J. & Stier P. (2004). M7: An efficient size-resolved aerosol microphysics module for
955 large-scale aerosol transport models. *Journal of Geophysical Research-Atmospheres.* 109(D22),
956 D22202, DOI: 10.1029/2003jd004485.
957 Vignati E., Karl M., Krol M., Wilson J., Stier P. & Cavalli F. (2010). Sources of uncertainties in
958 modelling black carbon at the global scale. *Atmospheric Chemistry and Physics.* 10(6), 2595-2611,
959 DOI: 10.5194/acp-10-2595-2010.
960 Wang Q., Jacob D. J., Spackman J. R., Perring A. E., Schwarz J. P., Moteki N., Marais E. A., Ge C., Wang
961 J. & Barrett S. R. H. (2014). Global budget and radiative forcing of black carbon aerosol: Constraints
962 from pole-to-pole (HIPPO) observations across the Pacific. *Journal of Geophysical Research:*
963 *Atmospheres.* 119(1), 195-206, DOI: 10.1002/2013JD020824.
964 Wang T. J., Zhuang B. L., Li S., Liu J., Xie M., Yin C. Q., Zhang Y., Yuan C., Zhu J. L., Ji L. Q. & Han Y.
965 (2015). The interactions between anthropogenic aerosols and the East Asian summer monsoon using
966 RegCCMS. *Journal of Geophysical Research: Atmospheres.* 120(11), 5602-5621, DOI:
967 10.1002/2014JD022877.
968 Wang X., Doherty S. J. & Huang J. (2013). Black carbon and other light-absorbing impurities in snow
969 across Northern China. *Journal of Geophysical Research-Atmospheres.* 118(3), 1471-1492, DOI:
970 10.1029/2012jd018291.
971 Warren S. G. & Wiscombe W. J. (1980). A model for the spectral albedo of snow. II: Snow containing
972 atmospheric aerosols. *Journal of Atmospheric Sciences.* 37, 2734-2745.
973 Wiedinmyer C., Yokelson R. J. & Gullett B. K. (2014). Global Emissions of Trace Gases, Particulate
974 Matter, and Hazardous Air Pollutants from Open Burning of Domestic Waste. *Environmental Science*
975 *& Technology.* 48(16), 9523-9530, DOI: 10.1021/es502250z.
976 Wofsy S. C., Team H. S., Cooperating Modellers T. & Satellite T. (2011). HIAPER Pole-to-Pole
977 Observations (HIPPO): fine-grained, global-scale measurements of climatically important atmospheric
978 gases and aerosols. *Philosophical Transactions of the Royal Society a-Mathematical Physical and*
979 *Engineering Sciences.* 369(1943), 2073-2086, DOI: 10.1098/rsta.2010.0313.
980 Ye H., Zhang R., Shi J., Huang J., Warren S. G. & Fu Q. (2012). Black carbon in seasonal snow across
981 northern Xinjiang in northwestern China. *Environmental Research Letters.* 7(4), 044002, DOI:
982 10.1088/1748-9326/7/4/044002.
983 Zhang Q., Jimenez J. L., Canagaratna M. R., Allan J. D., Coe H., Ulbrich I., Alfarra M. R., Takami A.,
984 Middlebrook A. M., Sun Y. L., Dzepina K., Dunlea E., Docherty K., DeCarlo P. F., Salcedo D., Onasch T.,

985 Jayne J. T., Miyoshi T., Shimono A., Hatakeyama S., Takegawa N., Kondo Y., Schneider J., Drewnick F.,
986 Borrmann S., Weimer S., Demerjian K., Williams P., Bower K., Bahreini R., Cottrell L., Griffin R. J.,
987 Rautiainen J., Sun J. Y., Zhang Y. M. & Worsnop D. R. (2007). Ubiquity and dominance of oxygenated
988 species in organic aerosols in anthropogenically-influenced Northern Hemisphere midlatitudes.
989 *Geophysical Research Letters.* 34(13), L13801, DOI: 10.1029/2007gl029979.
990 Zhang X. Y., Wang Y. Q., Niu T., Zhang X. C., Gong S. L., Zhang Y. M. & Sun J. Y. (2012). Atmospheric
991 aerosol compositions in China: spatial/temporal variability, chemical signature, regional haze
992 distribution and comparison with global models. . *Atmos. Chem. Phys.* 12, 779-799.

993

994 **TABLES**

995 *Table 1: Summary and description OsloCTM2-M7 experiments performed in this study.*

Experiment	Description
Baseline	Standard M7 OsloCTM2 simulation
CoatThick0.5	Required coating thickness reduced to 0.5ML
CoatThick1.4	Required coating thickness increased to 1.4ML
CoatThick2.3	Required coating thickness increased to 2.3ML
EmisTest	50% of biomass burning BC emitted directly in soluble accumulation mode
ConvBCi100	Hydrophobic BC removed by convective precipitation, 100% efficiency
ConvBCi20	Hydrophobic BC removed by convective precipitation, 20% efficiency
LSice12	Scavenging by ice in large-scale precipitation reduced from 100% to 20%
CombPert	LCice12 + ConvBCi20
NitCond	Aging by HNO3 condensation included
NitConcV2	As above, but excluding HNO3 produced by aqueous-phase N_2O_5 reaction
EmisSeasonality	Seasonality in domestic or agricultural waste burning BC emissions removed
EmisBCRUS	BC emissions in Russia replaced by Huang et al. (2015) inventory

996

997

998 *Table 2: BC lifetime and burden, and the change in global-mean RF, DRF and surface*
999 *temperature response from the baseline in each experiment.*

	Global				
	Lifetime	**Burden**	**ΔERFari**	**ΔRFari**	**ΔTS**
	[days]	**[Gg]**	**[mW/m^2]**	**[mW/m^2]**	**[mK]**
Base	6.0	133	-	-	-
CoatThick0.5	4.8	106	-26	-88	-14
CoatThick1.4	6.7	150	18	55	11
CoatThick2.3	8.3	185	52	166	32
EmisTest	5.9	131	-1	-7	-0.3
ConvBCi100	3.6	81	-49	-181	-25
ConvBCi20	4.8	107	-24	-91	-11
LSice12	6.6	147	15	46	8
Combpert	6.6	148	15	49	8
NitCond	4.9	109	-24	-84	-11
NitCondv2	3.9	87	-45	-157	-23

Atmos. Chem. Phys. Discuss., doi:10.5194/acp-2016-782, 2016
Manuscript under review for journal Atmos. Chem. Phys.
Published: 9 September 2016

Atmospheric Chemistry and Physics Discussions

1000

1001

1002

1003

1004

1005

1006

1007 **FIGURES**

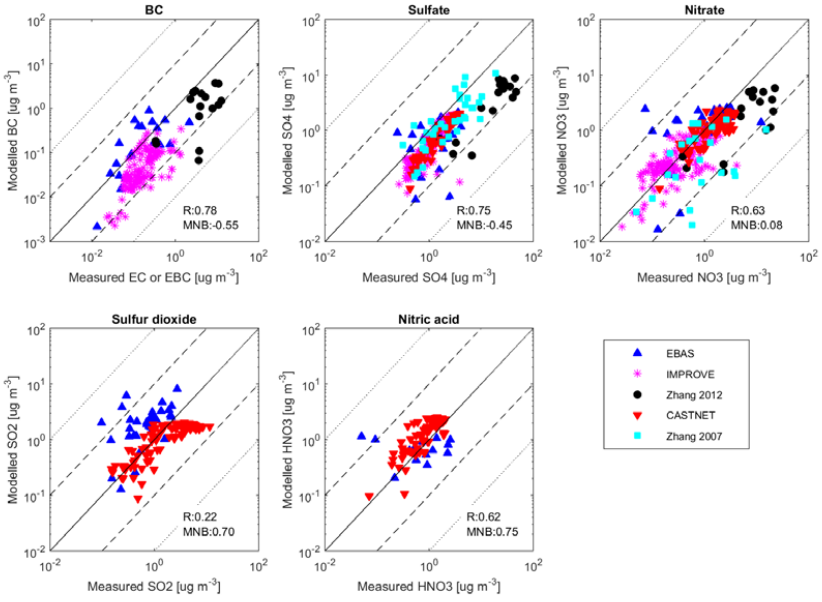

1008

1009 *Figure 1: Annual mean measured versus modelled BC, sulfate, nitrate, sulfur dioxide and nitric*

1010 *acid surface concentrations across Europe, North America and Asia.*

1011

Atmos. Chem. Phys. Discuss., doi:10.5194/acp-2016-782, 2016
Manuscript under review for journal Atmos. Chem. Phys.
Published: 9 September 2016

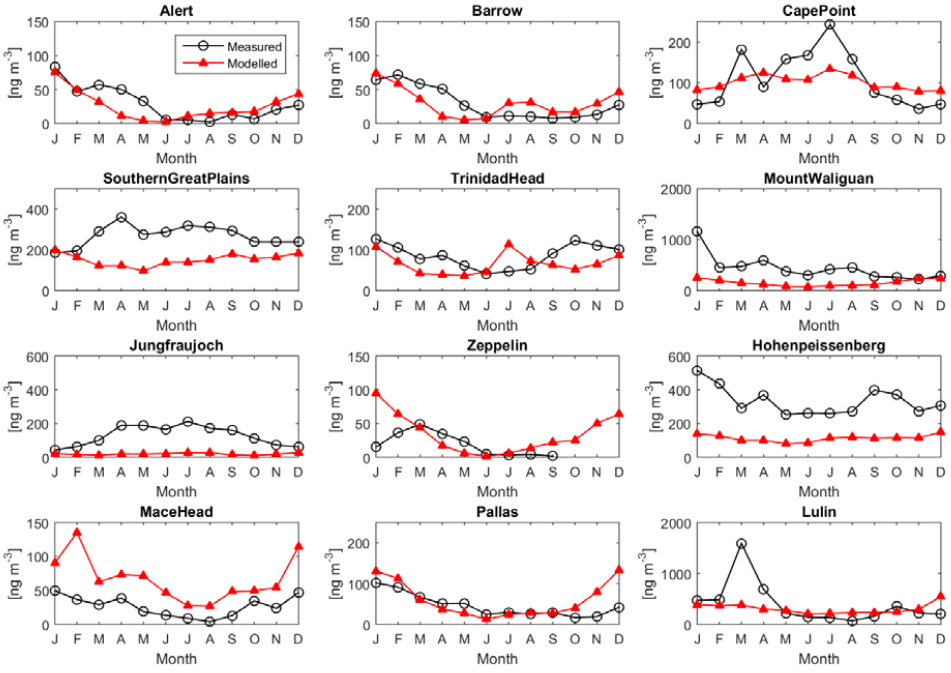

Figure 2: Monthly mean measured EBC versus modelled BC surface concentrations [ng/m3] averaged over 2008-2010 (data at Lulin only available for 2009-2010).

Atmos. Chem. Phys. Discuss., doi:10.5194/acp-2016-782, 2016
Manuscript under review for journal Atmos. Chem. Phys.
Published: 9 September 2016

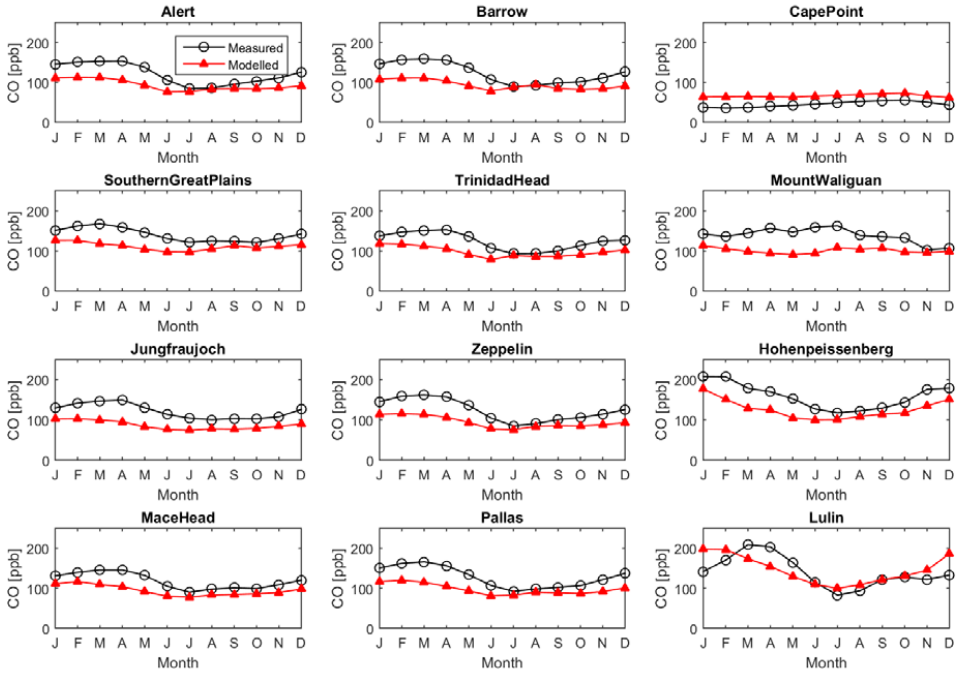

Figure 3: Monthly measured and modelled surface CO concentration [ppb] averaged over 2008-2010.

Atmos. Chem. Phys. Discuss., doi:10.5194/acp-2016-782, 2016
Manuscript under review for journal Atmos. Chem. Phys.
Published: 9 September 2016

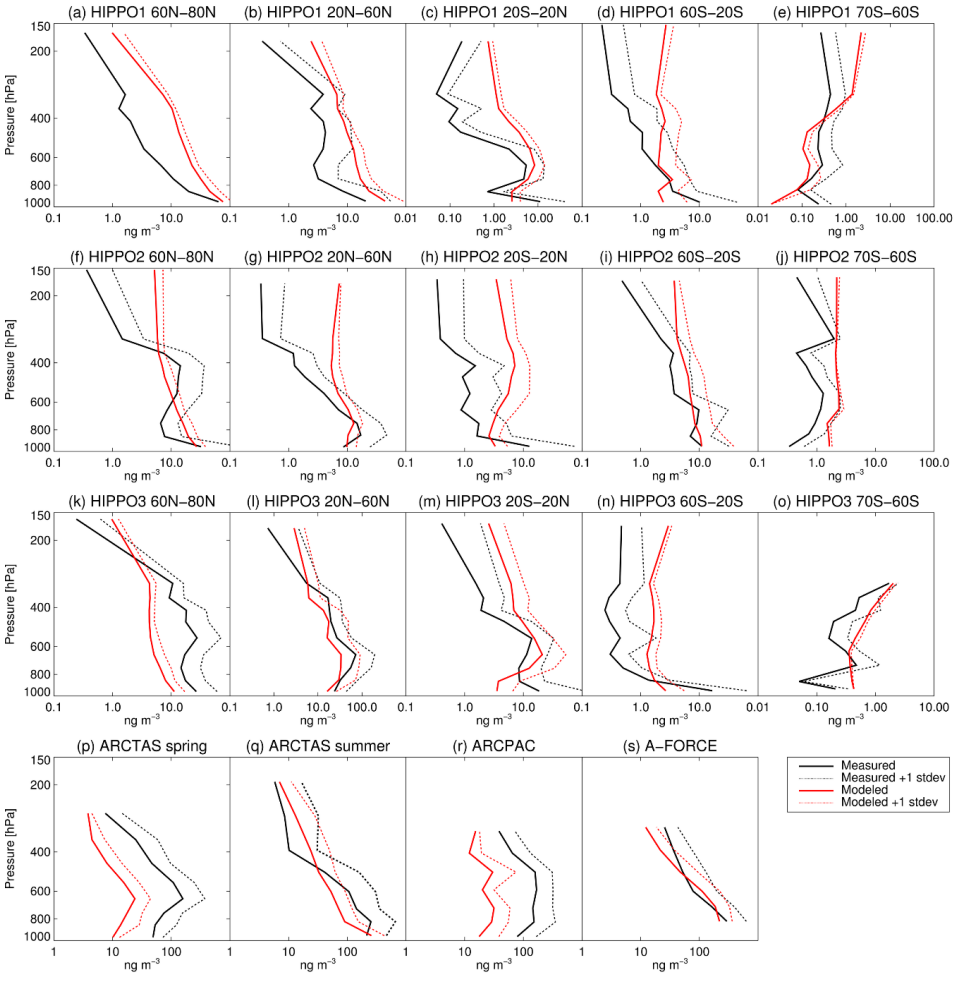

Figure 4: Comparison of modeled vertical profiles of BC with measured rBC from six fligh campaigns: (a)-(o) HIPPO 1-3, averaged over five latitude bands, (p)-(q) ARCTAS, spring and summer, (r) ARCPAC and (s) A-FORCE. Solid lines show the average of observations and model results binned in 100 hPa invervals (25 hPa for HIPPO data between 400 and 200 hPa), while dashed lines show the standard deviation in each interval.

Atmos. Chem. Phys. Discuss., doi:10.5194/acp-2016-782, 2016
Manuscript under review for journal Atmos. Chem. Phys.
Published: 9 September 2016

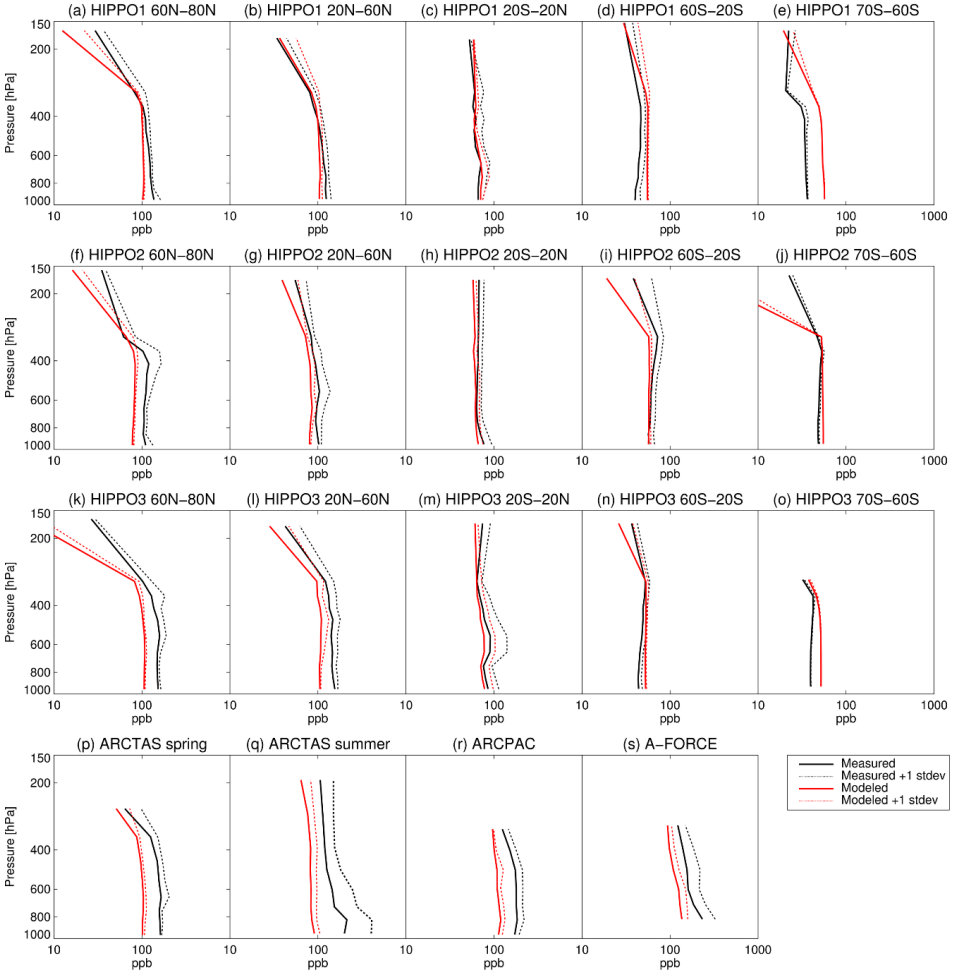

Figure 5: same as Fig. 4, but for CO.

Atmos. Chem. Phys. Discuss., doi:10.5194/acp-2016-782, 2016
Manuscript under review for journal Atmos. Chem. Phys.
Published: 9 September 2016

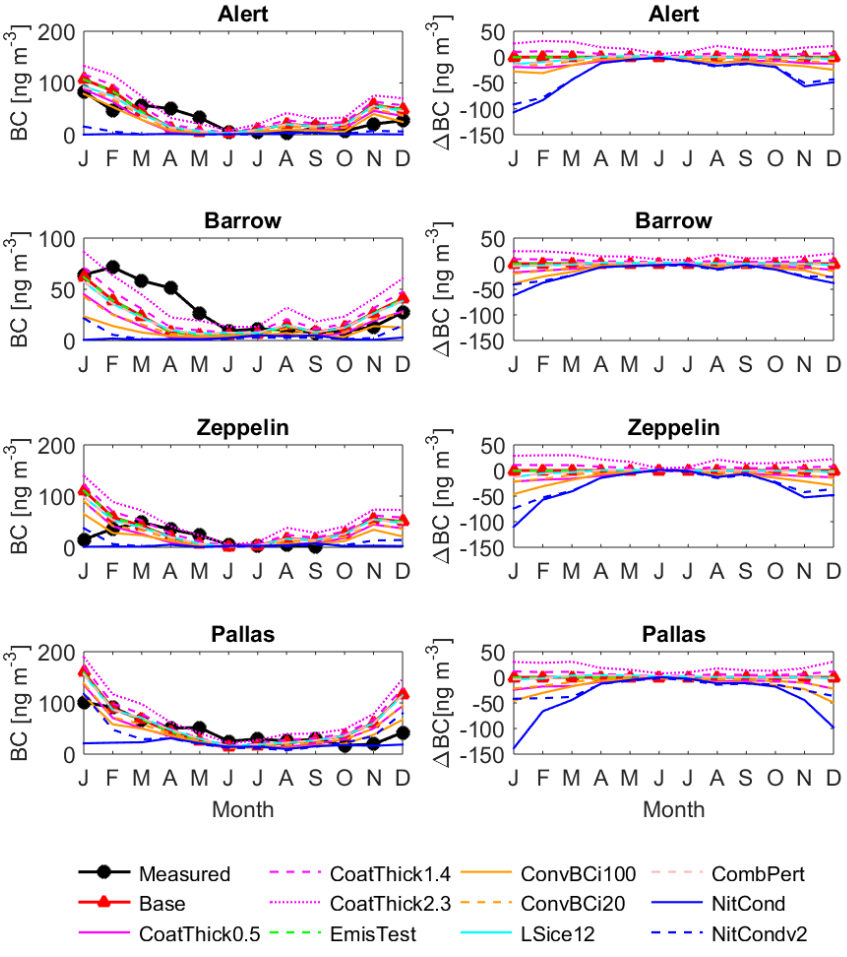

Figure 6: Monthly surface concentrations of BC at Arctic stations in 2008: measurements versus baseline and sensitivity simulations (right column) and difference between each sensitivity simulation and the baseline (left).

Atmos. Chem. Phys. Discuss., doi:10.5194/acp-2016-782, 2016
Manuscript under review for journal Atmos. Chem. Phys.
Published: 9 September 2016

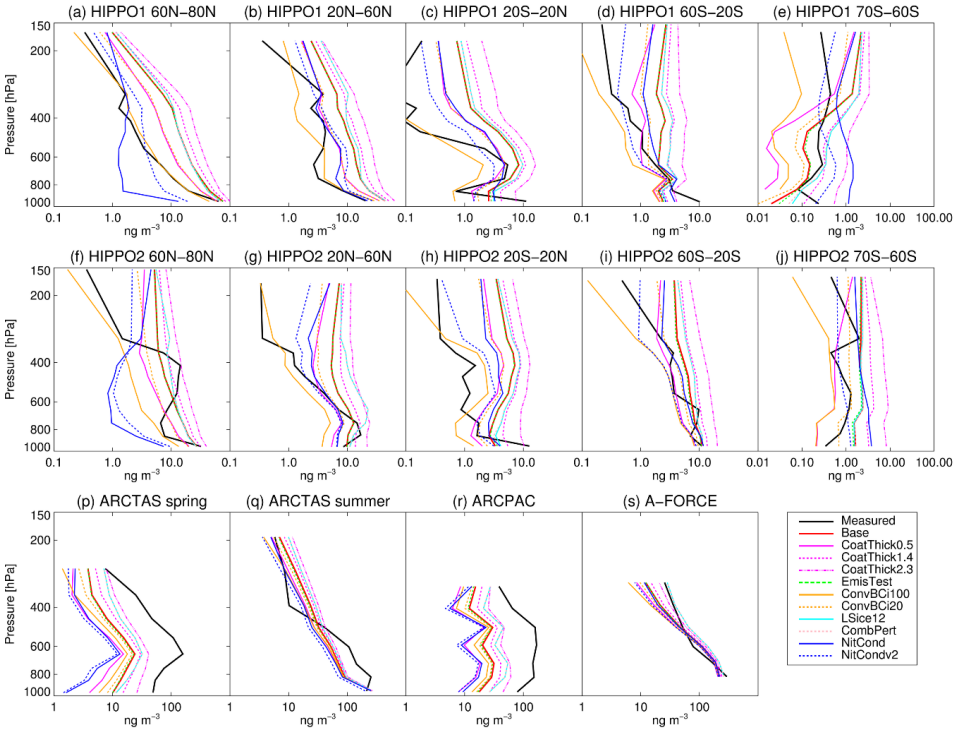

Figure 7: Vertical profiles of BC in the control and sensitivity runs compared to flight campaigns.